Seismic Characterization of Abandoned Mine Overburden Along U.S. Highway 69 North of the Kansas/Oklahoma State Line

Richard D. Miller, Joseph M. Fontana, Sarah L.C. Morton,
Shelby L. Peterie, Daniel Z. Feigenbaum, Julian Ivanov,
Brett Bennett, Brett Wedel, Joe Anderson, Tom Stevens, and Andy Banks

Kansas Geological Survey
1930 Constant Avenue
Lawrence, KS 66047

Report to

Robert Henthorne, Chief Geologist
Materials and Research Lab
Kansas Department of Transportation
2300 Van Buren
Topeka, KS 66611
Ph (785) 291-3860

December 2016

Kansas Geological Survey Open-File Report 2024-5

Seismic Characterization of Abandoned Mine Overburden Along U.S. Highway 69 North of the Kansas/Oklahoma State Line

Summary

Multiple seismic methods were used to characterize the overburden above the drill-confirmed roof of an abandoned lead-zinc mine (Webber-Barr Mine) below about a half-mile of U.S. Highway 69 near the Kansas/Oklahoma state line in Treece, Kansas, which is part of the Tri-State Mining District. The top of the Webber-Barr Mine is located at depths ranging from 190 to 270 ft and has a highly altered cherty limestone roof. Mine maps indicate unsupported roof spans of greater than 600 ft in some areas. Based on geologic reports and historical records, roof rock strength may be compromised by vertical fractures and faults that extend from the mine roof to within the overlying shale bedrock. Unpredictable roof rock failure could result in rapid vertical void migration extending to the surface of the highway, and is therefore a potential risk to public safety.

A reliable measure of seismic velocities as a function of depth can be a comprehensive and accurate method for appraising overburden characteristics along the undermined stretch of highway. Shallow seismic-reflection methods have proven effective for identifying void geometry and interrogating overburden materials to qualitatively evaluate subsidence potential and future extent of surface deformation (Steeples and Miller, 1990; Miller et al., 1997; Miller, 2007; Miller et al., 2006; Lambrecht, 2006; Judy, 2015). With shear velocity directly related to stress through the shear modulus, lateral or time variations in stress (symptom of changes in rock strength or differential changes in force on rock units) can be estimated from laterally continuous measurements of shear velocity in rocks using various seismic methods. Local increases in shear velocity, and thus decreases in the ratio of compressional- to shear-wave velocity (Vp/Vs) calculated from reflection interval velocities, can be equated to increased stress associated with increases in overburden roof load. Relative shear velocity lows may be associated with reduced stress within roof rock due to collapse or changes in roof support.

In 2015 and 2016, compressional- and shear-wave seismic-reflection surveys were collected along the southernmost 1.5 miles of U.S. Highway 69 in Kansas to evaluate the methods' effectiveness in appraising the condition of the mine's roof rock and overburden and to establish a potential baseline for establishing change in the future. Due to local faulting and the fractured cherty limestone overburden at this site, extensive preprocessing and data conditioning were essential in producing meaningful images of the subsurface. Delineating reflections from coherent noise and scatter allowed interpretation of the mine roof, likely support features (pillars), and surrounding structures that could all be correlated with drill data and other geophysical data. Interpretation of the P-wave reflection data primarily focused on areas above the mine void and the full depth interval above competent rock. S-wave interpretations are influenced by the rock matrix and therefore voids and fluid are invisible to that type energy. S-wave energy for this study was limited to coherent, high-amplitude reflections that are associated with the limestone roof rock and overburden of the mine.

Vp/Vs values calculated from the two high-resolution seismic datasets were used to estimate the integrity and consistency of the mine's roof rock and overburden. Rock interpreted to have a slightly higher Vp/Vs in various locations across the profile are likely a result of highly altered limestone units effecting a drop in shear-wave velocity. None of the variability in Vp/Vs was sufficient to elevate concern about an eminent collapse. Well data from boreholes acquired in a previous study along the extent of the mine under the highway, were tied to the seismic lines and used to corroborate the Vp/Vs.

The multichannel analysis of surface waves (MASW) method was used in June 2015 and 2016 to produce a 2-D shear-wave velocity (Vs) map of sufficient quality to provide insights into material stiffness (i.e., modulus) and very general perspectives of trends in stratigraphic layering. This surface-wave inversion technique isolated arrivals with low enough frequency content to successfully sample to depths between 70 and 80 ft below ground surface throughout the entire survey line. No unusual variation in shallow (< 80 ft) soil and rock structure was observed consistent with impending roof-structure failure at these depths at the time of the survey.

Passive three-component, single-station seismic data were also collected at wells 1-14 to measure the natural resonance frequency of the soil overburden using the horizontal-to-vertical spectral ratio (HVSR). Given known depth-to-bedrock measurements, the average shear-wave velocity of the soil overburden can be estimated using resonance frequency values in the presence of a 2:1 velocity contrast between soil and bedrock. The results of these data will supplement the observed silty clay and shale boundary in the MASW results based on the state of the shale weathering. Weathered materials yield a lower shear-wave velocity than stiffer, firm materials, and if the weathering is more severe than anticipated, it can be more susceptible to rapid failure.

Introduction

Hundreds of surface collapse features have been mapped in the Tri-State Mining District of Kansas, Missouri, and Oklahoma (Luza, 1986; McCauley et al., 1983). Over 300 Pb-Zn mine collapse structures and sinkholes have developed in southeastern Kansas alone, with 17 documented in the Treece area (Figure 1). Considering the geology and mining history around Treece, it is prudent to monitor the condition/fitness of overburden rock in areas known to be undermined and where public safety could be at risk.

The north/south trending U.S. 69 highway passes less than a half-mile east of the town of Treece and directly over two known mined areas (Webber-Barr Mine and Foley Mine), with the northernmost undermined area having a documented history of overburden failure (Foley Mine) that has required surface repair within the highway right of way (Williams and Fredericksen, 1985) (Figure 2). However, it is the Webber-Barr Mine, which underlies about a half-mile stretch of the highway between one-quarter and three-quarters of a mile north of the border that has been suggested to possess the greatest potential threat to highway stability in this area (Williams and Fredericksen, 1985).

Figure 1. Mine collapse northwest of Treece, Kansas (photo from *Wichita Eagle*, 2009).

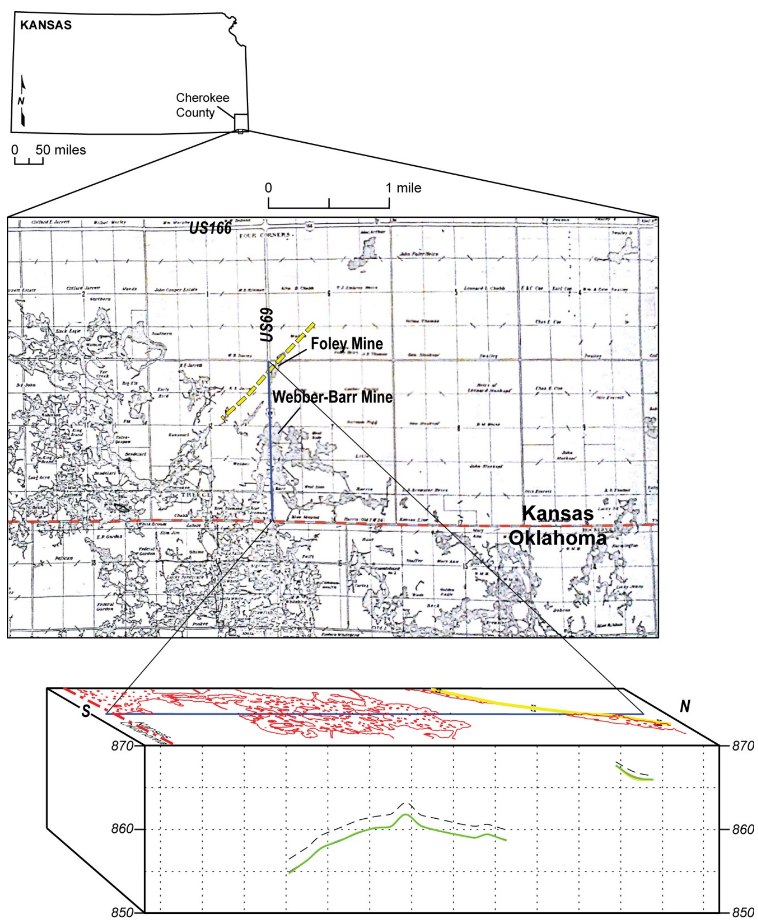

Figure 2. Mine map from study area. Surface elevation map with five repeat surveys superimposed, demonstrating that there has been no ground movement since the original baseline survey. The yellow line is an inferred fault associated with the southern flank of the Miami trough.

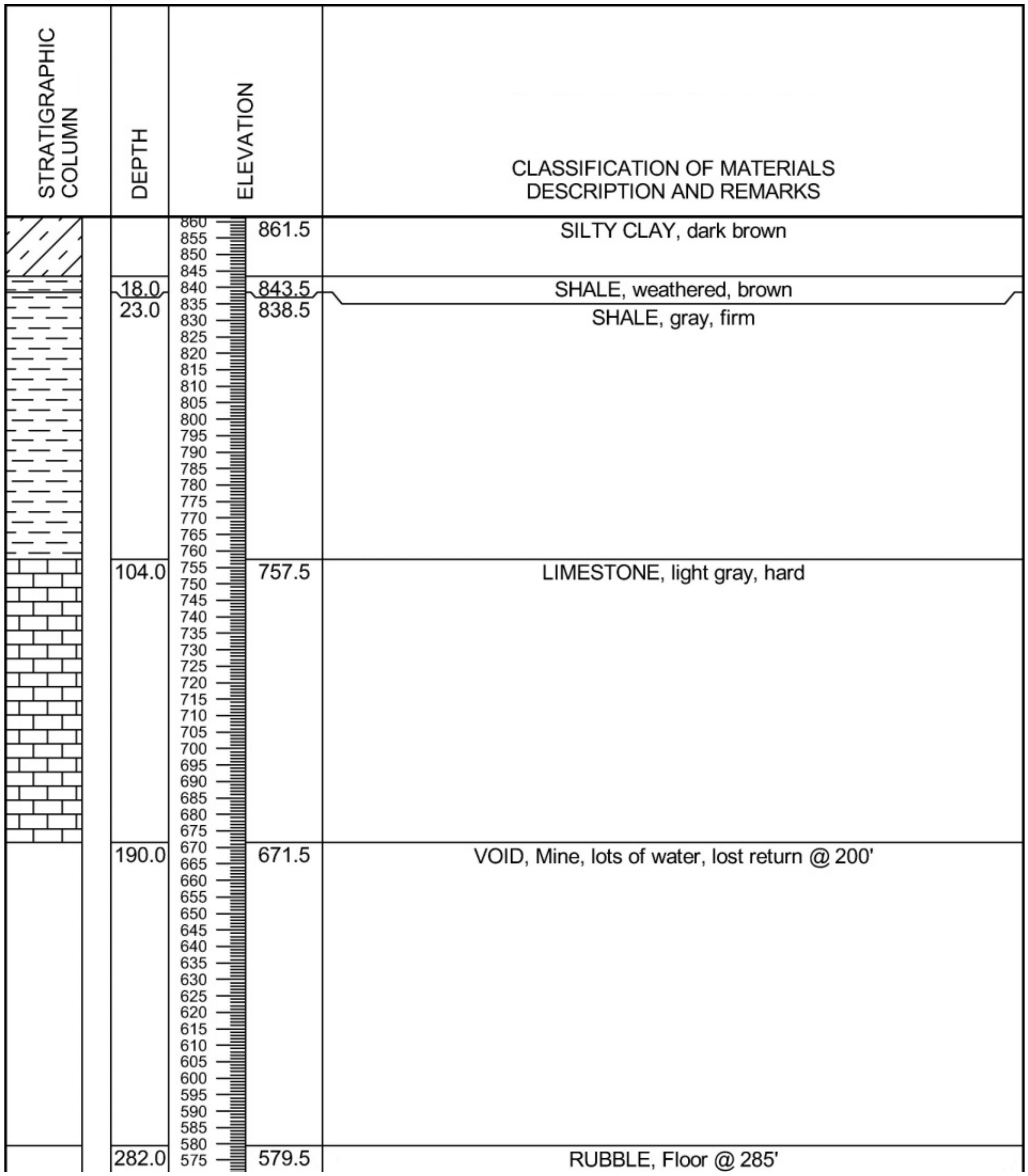

Figure 3. Boring log provided by KDOT from along proposed survey line. This location is characterized by a more than 90-ft-high, water-filled void/room.

Unlike the Foley Mine with its shale roof rock, the Webber-Barr Mine can be characterized by a highly structurally altered cherty limestone roof (Williams and Fredericksen, 1985). The Webber-Barr Mine roof is very irregular and has been encountered along the highway at a depth from around 190 ft to over 250 ft below ground surface (BGS) (Figure 3) (Table 1). Drilling confirms the mineworks are water filled, with some rooms nearly 100 ft tall (KDOT, 2009). One of the biggest safety concerns is the presence of large unsupported roof spans (> 600 ft if all the pillars are present), as indicated on the mine maps. These characteristics make the first 1.25-mile stretch of U.S. 69 north of the Oklahoma border a priority concern for ground stability and therefore a potential risk to public safety.

Table 1. Well locations along U.S. Highway 69

Well	MASW Station	P-wave Reflection Station	S-wave Reflection Station	Comments
1	999	1187	1190	Mine detected 230 - 242 ft
2	1057	1214	1218	Mine detected 230 ft
3	1107	1238.5	1243	Mine detected 240 - 308 ft
4	1157	1262.5	1267	Mine detected 273 - 294 ft
5	1195	1282	1286.5	No mine detected
6	1266	1311	1316	Mine detected 190 - 280 ft
7	1313	1335.5	1340	Mine detected 198 - 278 ft
8	1363	1368	1364	Mine detected 244 - 318 ft
9	1413	1384.5	1389	No mine detected
10	1463	1408	1413	No mine detected
11	1519	1436	1442	Mine detected 290 - 315 ft
12	1563	1456	1462	No mine detected
13	1614.5	1481	1487	No mine detected
14	1663	1505	1510	Mine detected 285 - 295 ft

In an attempt to monitor the fitness of the overburden beneath the road surface, a series of boreholes were drilled in 2002 in support of crosshole seismic investigations (Figure 3). These studies were designed to determine the initial fitness of the overburden at that time with repeat surveys intended to monitor change that might be a precursor to overburden failure. These seismic monitoring boreholes penetrated the highly altered cherty limestones of the Boone Formation and were subsequently lost due to borehole collapse. Rocks in the Boone Formation above and near the mine are sufficiently altered/deformed that in many places they lack the competency necessary to maintain the integrity of the seismic monitoring boreholes.

Underground workings in the Picher-Treece area are within highly altered cherty limestones with pronounced faulting and high-amplitude, high-frequency folding (McKnight and Fischer, 1970). Mineralized intervals mined in the Treece area generally range from 200 to 600 ft BGS (Figure 4). Ore deposition was accomplished through hydrothermal solutioning into structurally altered and fractured permeable rocks. As a result of the highly altered nature of these host rock, both mine geometry and roof properties vary significantly from mine to mine and even within a single mine drift. The highly altered rocks observed in mine drifts as well as those encountered in vertical shafts between the mined intervals and ground surface lack the strength found native to these overburden rocks outside this structurally disturbed area. Mineralization with economic ore deposits are generally bounded on the north by the Miami trough. The Foley Mine is on the steep southern flank of the syncline.

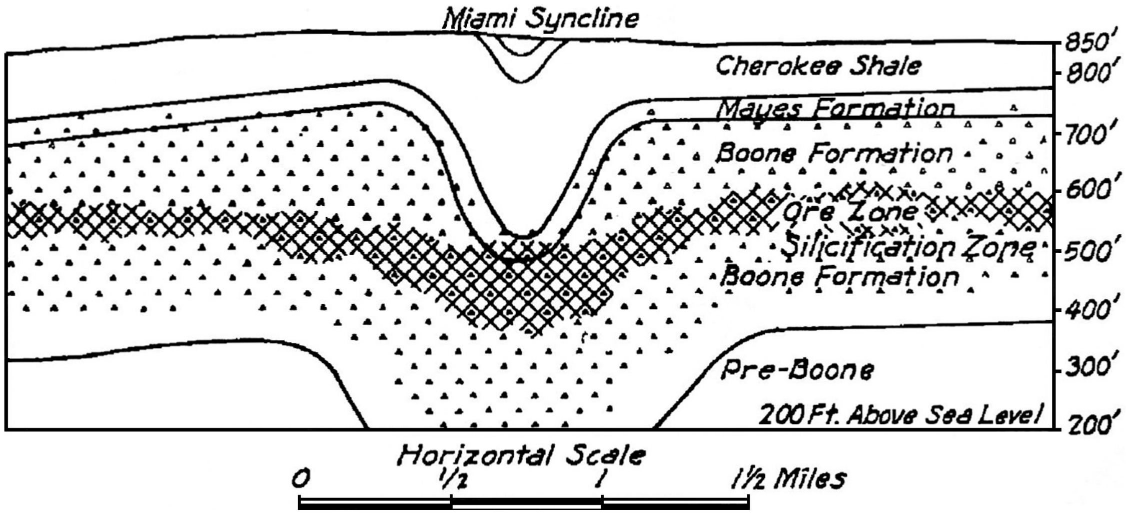

Figure 4. Cartoon from Weidman (1932). The ore zone and silicification zone are present together and are associated with highly fractured and faulted areas. On the southern side of the Miami Syncline the ore zone had economic quantities of ore at depths from between 200 and 600 ft, with most around Treece in the upper 200 ft of that zone.

Roof rock strength is highly compromised in some areas where vertical fractures or faults extend from the mine roof to the base of the shale, or in some cases these breaks in rock coherency extend to near the bedrock surface. Slump pipes are routinely observed in rock faces exposed in mines within a few thousand feet of the Miami trough (syncline) (Weidman, 1932) (Figure 5). Mined areas of concern along U.S. Highway 69 are bounded by the Miami trough on the north and extend south to the state line (actually further south than the state line, but for our purposes our responsibility ends at the state line) (Figure 6). Slump features, as described previously, are fault controlled and generally defined by an irregular, cylindrical mass several hundred feet in diameter down-dropped several tens of feet. These slump features extend into the highly altered overburden prevalent in the Treece area. The fault zones that bound these slump pipes gradationally transition into highly brecciated zones. The block central to each of these slump pipes is generally tilted and compressed with some in-place chert shattering but lack extreme brecciation and gouge routinely observed in fault zones. Slump pipes are commonly found in this area with extensive mineralization.

It is the hidden nature of slump pipes generally masked by the shale portion of the overburden that represent some of the greatest risk to surface structures. Unlike gradational surface collapse at the Foley Mine, which occurred over a period of almost 40 years and was driven by water contact with the shale roof rock and the resulting gradual degradation, collapse of the Webber-Barr Mine could be catastrophic (Williams and Fredericksen, 1985) and, depending on the bulking factor, could result in the formation of a sinkhole in minutes that possessed sheer sides and was over 50 ft deep. High volumes of water and a shale roof rock in the Foley Mine made the roof rock in that mine susceptible to failure from gradual stoping of the shale and void migration into the overburden. The subsurface void (mine drift) eventually migrated to the ground surface in the form of an ever widening depression that naturally arrested once the mine

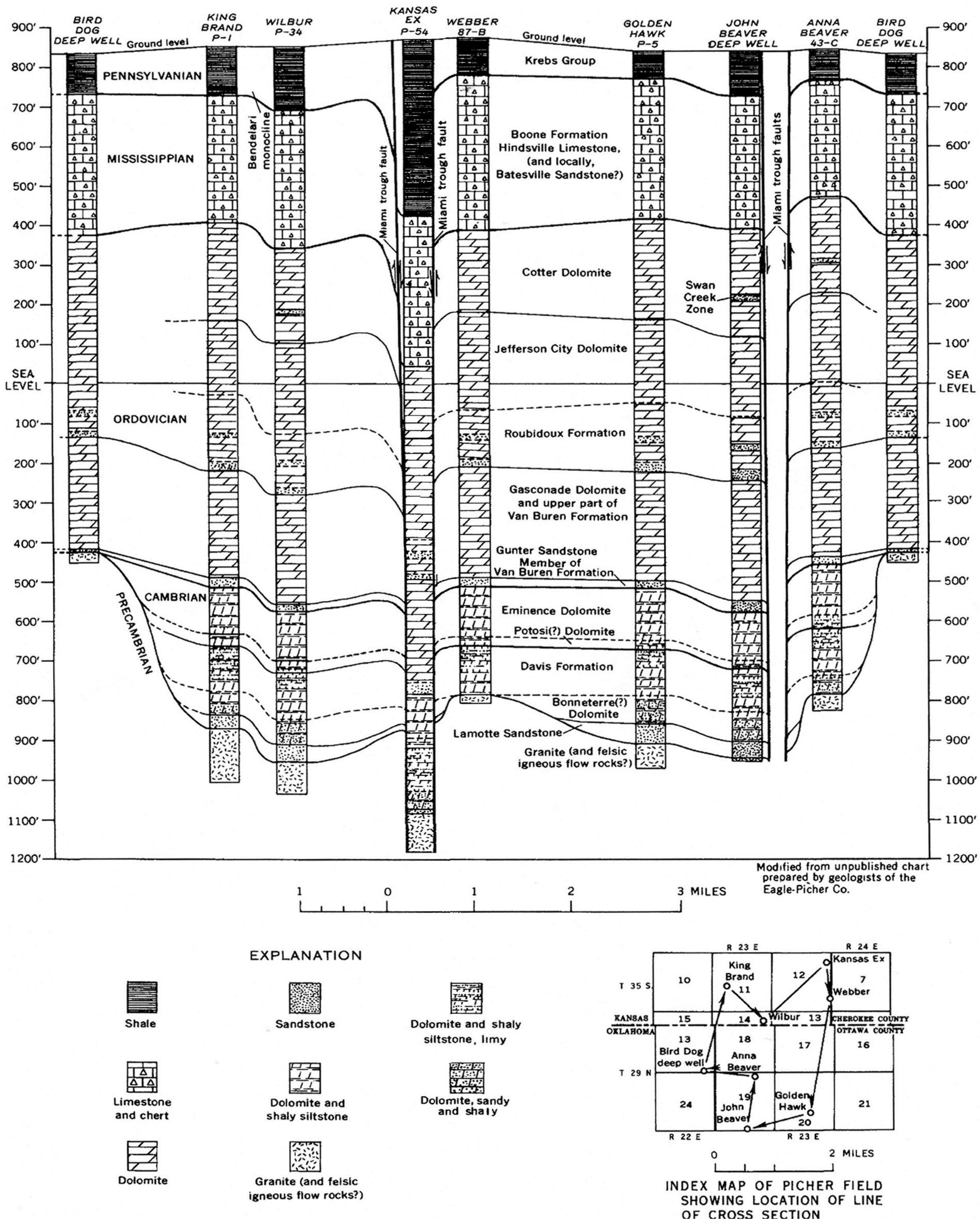

Figure 5. Borehole lithology from McKnight and Fischer (1970). The Miami trough was clearly encountered in boring labeled Kansas EX.

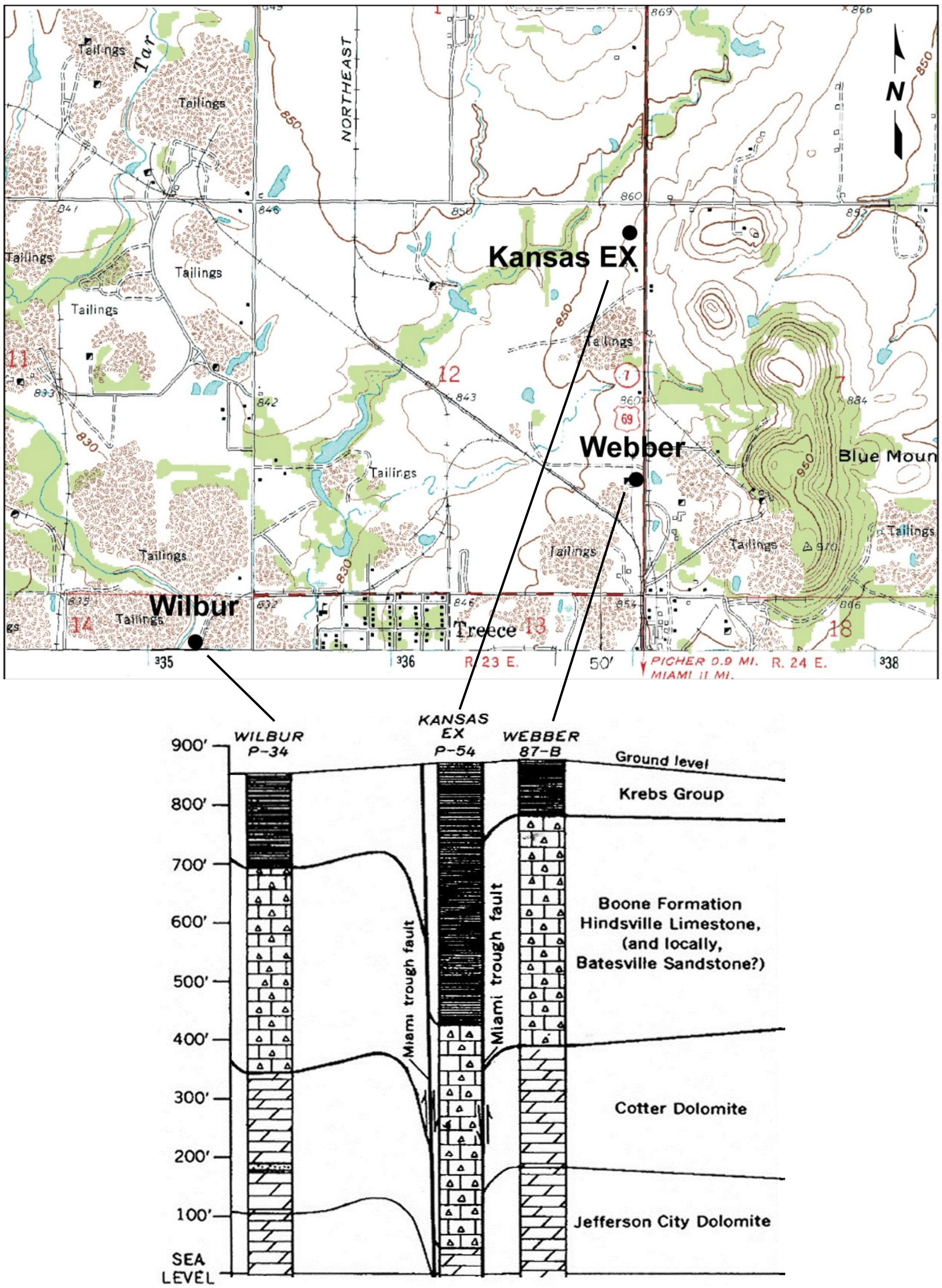

Figure 6. Site map of boring locations within the study area. In Kansas EX, the base of the trough is around 400 ft below ground surface, making the trough itself around 300 ft deep. The south-bounding Miami trough fault is interpreted on the elevation monitoring survey in Figure 2.

void filled. Surface remediation was limited to backfilling. This scenario is unlike the way a collapse of the Webber-Barr Mine will progress.

Mines in this area that are overlain by highly altered cherty or dolomitic limestones, such as encountered in the Webber-Barr Mine (Williams and Fredericksen, 1985), can experience roof rock failure along structurally weak zones, such as slump pipes. Slump pipes represent existing vertical zones of weakness that can facilitate rapid upward void migration to the ground surface. With the high strength of the unaltered rocks of the Boone Formation, once failure occurs along these fracture or fault edges of structures such as slump pipes, the potential for catastrophic formation of a steep-sided, deep sinkhole is high. The steep-sided nature of these sinkholes is related to the strength of the rocks that constitute the sidewalls of a sinkhole. Once subsidence has halted due to void stability, the sidewalls of the sinkhole will equilibrate with resting slope angles defined by the angle of draw (Miller, 2007). Slump pipes have been mapped in outcrops of the Boone formation in areas east and southeast of the study area (McKnight and Fischer, 1970).

Unexpected, catastrophic failure of near-surface materials represents a potential risk to life and property in a wide variety of settings. All subsurface voids have the potential for roof failure, at least partial collapse of overburden, and migration, some reaching the ground surface. Vertical migration of a void to the ground surface is controlled by void location, geometry, and properties of overlying rock. Once the characteristics of a void and overburden are known, the rate of migration and size of the resulting surface subsidence feature can be estimated from incorporating the void characteristics with angle of draw (calculated using overlying rock properties) and competency of the overburden. Shallow seismic-reflection methods have proven effective throughout Kansas identifying void geometry and interrogating overburden materials (Miller, 2007) such that void properties and characteristics of the overburden can be sufficiently appraised to qualitatively evaluate subsidence potential and future extent of surface deformation.

A P-wave high-resolution seismic-reflection profile, coincident S-wave high-resolution reflection profile, a continuous MASW survey, and a set of H/V passive seismic soundings were acquired along U.S. 69. Coverage generally extended from near the Oklahoma/Kansas state line north to just beyond the mapped location of the Foley Mine and beyond the axis of the Miami trough (Figure 7). A representative common midpoint stack of the P-wave data was produced by relying on detailed velocity analysis with surface-consistent statics to optimally stack coherent reflections. Correlating the reflections to likely reflectors allowed for a reasonably confident interpretation of the trough and mine. The S-wave survey was conducted over the same stretch of highway to allow coincident correlation of reflectors, to characterize the strength of over-burden, and identify areas of potentially elevated stress. A high percentage of relatively higher velocity surface waves drastically reduced the optimum reflection window between first arrivals and surface waves and made for challenging interpretation of reflections. Detailed muting and filtering, along with an extensive and spatially dense velocity model, were crucial in delineating the subsurface for a correct final stacked section. Vp/Vs was calculated using the interval velocities from the two high-resolution seismic datasets, to determine if large changes in lateral rock properties were present in the mine overburden. Well data was tied to the seismic lines and Vp/Vs to confirm the mine location.

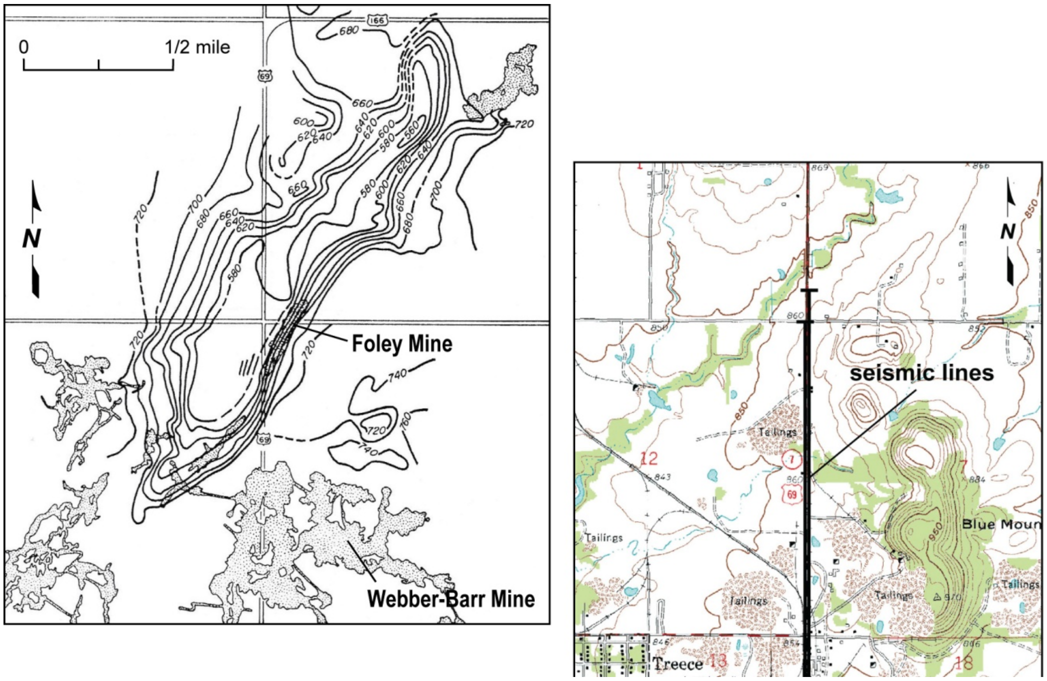

(a) (b)

Figure 7. (a) Contours along the southern flank of the Miami trough, coincident with U.S. Highway 69, are tightly spaced and indicative of a relatively narrow fault zone (Hambleton et al., 1959). (b) The seismic survey will cross the trough at around a 45-degree angle from orthogonal, so some smearing of the structure will likely result.

Geologic Setting

Rock exposures in outcrop at various locations around Cherokee County are principally Mississippian and Pennsylvanian limestone and shale, with alluvial silts, sands, clays, and gravels from the Quaternary making up the principle shallow sediments within stream and river valleys (Figure 8). Surface exposure of thin sections of bedded Mississippian and Pennsylvanian strata appear relatively flat and, from drill data, overlay an irregular Precambrian basement surface at a depth of around 1800 ft BGS near the northern end of the seismic lines (Figures 5 and 7). The Mississippian limestones and cherts exposed in Cherokee County are associated with the Ozark Plateau and are a primary constituent of the Tri-State Mining District.

The Lower Mississippian age Boone Formation contains the mineralized zone and associated mine voids of interest in the Treece area. The Boone Formation sits disconformably on top of the Chattanooga Shale of Late Devonian and Mississippian (Kinderhook) age and includes limestones of the Osage and Meramec. These predominantly cherty limestones include the St. Joe Limestone Member, Reeds Springs Limestone Member, Burlington Limestone, Keokuk Limestone, Warsaw Limestone, Salem Limestone, St. Louis Limestone, and the Ste. Genevieve Limestone. The Boone is composed of fossiliferous limestone, cotton rock, and chert (McKnight and Fischer, 1970). The chert generally occurs in nodules and interbeds ranging in thickness from a few inches to 60 ft. Ore host rock in the Boone Formation in the area around Treece ranges from 350 to 400 ft thick.

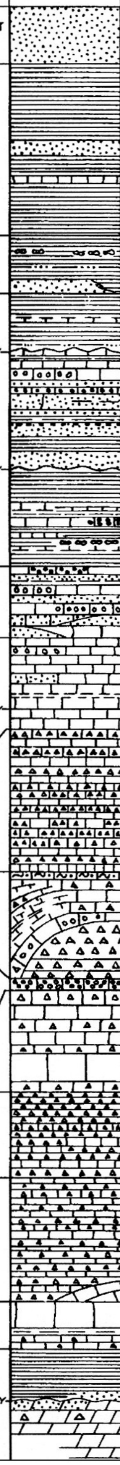

System	Series	Group, formation or member		Columnar section	Thickness (feet)	Description
PENNSYLVANIAN	Des Moines	Krebs Group	Bluejacket Sandstone Member (of Boggy Formation)		15-60	Brown to buff sandstone.
			Savannah Shale Doneley Limestone Member of Branson, 1954		120 ±	Black and gray fissile shale, a little sandstone, thin black fossiliferous limestone (Doneley Member), thin coal and underclay seams (Branson, 1955).
			McAlester Shale Warner Sandstone Member		30 ± 0-20	Black fissile shale with clay ironstone concretions, sparse siltstone, thin coal and underclay; brown coarse-grained sandstone (Warner) at base (Branson, 1955).
			Hartshorne Formation UNCONFORMITY		0-50	Dark-gray to black fissile shale, subordinate siltstone, sparse calcareous clay ironstone, and thin coal seams with underclay (Branson, 1955).
	Morrow	Hale Formation UNCONFORMITY			0-83+	Alternating brown to black carbonaceous and locally ferruginous sandstone, dark shale, and fossiliferous bituminous limestone, partly oolitic.
MISSISSIPPIAN	Chester	Fayetteville Shale			0-70	Black, bluish-gray, and greenish fissile or limy shale with local ironstone concretions, subordinate gray and brown to purplish crinoidal limestone, part bituminous, part oolitic.
		Batesville Sandstone			0-70	Gray crinoidal to dense limestone, commonly oolitic, buff sandstone and green shale, interbedded.
		Hindsville Limestone UNCONFORMITY			0-85 ±	Gray crinoidal to dense limestone, commonly oolitic, locally cherty, a little sandstone and green shale.
	Meramec	Quapaw Limestone			0-31+	Gray medium- to coarse-grained crinoidal limestone.
		Boone Formation	Moccasin Bend Member		0-140	Alternating chert and fine- to medium-grained brown limestone, some cotton rock; chert conspicuously brown and blue in lower part, paler above.
			Baxter Springs Member		0-5 0-51 0-60	At base, bedded to massive pale chert or cotton rock, glauconitic at base (L bed); overlain and overlapped regionally by crinoidal glauconitic limestone and variegated chert, the limestone locally shaly or containing glauconitic oolite and phosphate nodules (K bed); topped by thin phosphatic and highly glauconitic crinoidal limestone containing variegated and, in part, very dark chert (J bed).
			Short Creek Oolite Member DISCONFORMITY		0-10	Brown oolitic limestone, only slightly glauconitic.
	Osage		Joplin Member		0-100	Gray crinoidal limestone and nodular or bedded chert; chert-free ledge near base.
			Grand Falls Chert Member		25-95	Pale chert, cotton rock, and subordinate brown fine-grained limestone.
			Reeds Spring Member		70-105	Blue, gray, and brown chert alternating with gray and brown fine-grained limestone; crinoidal bioherms locally at base.
			St Joe Limestone Member		10-32	Gray to pink crinoidal limestone with massive ledge at top and greenish shaly zone below middle; sparse blue to gray chert.
MISSISSIPPIAN AND DEVONIAN	Kinderhook and Upper Devonian	Chattanooga Shale UNCONFORMITY			0-50	Black fissile shale, bleached greenish or yellow at top; locally a few inches of coarse-grained white sandstone at base.
ORDOVICIAN	Lower Ordovician	Cotter Dolomite			26+	Gray to brown dolomite, fine-to medium-grained, locally sandy; a little chert, in part oolitic.

Figure 8. Stratigraphic column from McKnight and Fischer (1970). Based on boring data, the bedrock in the study area is likely Savannah Shale.

Overlying the Boone is the Chester Series, which includes three undifferentiated formations that grade from predominantly limestone to sandstones and shales of the upper Mississippian (Seevers, 1975). The Quapaw Limestone is reported to represent the top of the Boone and basal contact for the Pennsylvanian. It is known to be discontinuous across the Tri-State Mining District and not observed in borings in the study area. Rocks of the Mississippian Chester Series transition to the lower Pennsylvanian Morrow rocks, which in this area includes sandstones, dark shales, and bituminous limestones of the Hale Formation. In Kansas nomenclature these rocks would likely fall within the Kearny Formation.

The Krebs Group in Oklahoma, which includes the Krebs Formation as it is defined in Kansas, is the start of a major transition into the shale and coal-rich lower Cherokee Group. The Bluejacket Sandstone marking the top of the Krebs Formation is not present at this site and therefore the shale and coal packages in the lower half of the Krebs Formation represent bedrock along the proposed seismic profiles.

A dominant structural feature in this area, and one that clearly and strongly influenced mineralization and resulting mines beneath the highway, is the Miami trough. The Miami trough is a combination of syncline and graben. The inferred location of the Miami trough was obliquely intersected by the northern end of the seismic profile (Figure 7). The axis of the trough is approximately NE/SW and bounds the northern extent of mineralization in the Treece area. The trough extends over 40 miles, and where the seismic line is proposed to cross the trough it is around 1000 ft wide and 300 ft deep.

Of particular concern was the high number of slump pipes reported to be within a half-mile or so of the Miami trough (McKnight and Fischer, 1970). Slump pipes are fault controlled, down-dropped blocks that are problematic when encountered in a mine's roof rock. In this area the Webber-Barr Mine is located in an area known to have a high concentration of slump pipes. Most faults in the area not related to slump pipes run nearly parallel to the Miami trough. Faults mapped in mines around the area tend to vary only slightly in orientation and offset, with most less than 1000 ft in length.

Mineralized rocks were originally fractured along curvilinear vertical zones coincident with extensive joint systems, and it was these highly fractured zones that provided the access for mineralized solutions to infiltrate the rock. These joint systems have an extremely high correlation to tectonic breccias that formed as a result of plastic deformation during differential horizontal slippage that occurred between more competent bounding limestone during the warping process that resulted in the Miami trough as well as other minor structures.

Ore deposits in the Treece area are generally in the upper half of the Boone Formation and with occasional and minor extension into the overlying Mayes Formation (McKnight and Fischer, 1970) (Figure 8). The ore is generally in economic concentrations within these formations when associated with highly silicified and dolomitized zones. The mineable deposits are found in various irregular shapes but generally characterized as flat when they have a flat top and bottom that is generally parallel to bedding; can range from 20 ft to 100 ft wide; vertical (10 to 15 ft wide and up to 150 ft or more in height) runs have steep walls and are generally associated with faults or fissures; and pockets—which are small ore bodies generally separated from a main ore body by a minimally mineralized zone. Ore accumulations in these mineable bodies are generally conglomerated with broken and brecciated angular blocks of fractured rock.

Structural features mapped in this area formed at different times. A key player in this study is the Miami trough, which was principally active during the Morrow, with deformational enhancement of post-Cherokee age rocks. Most likely the tectonic breccias and joint systems occurred during Late Pennsylvanian with no significant deformation occurring since Cretaceous when the ore was likely deposed.

Seismic Interrogation and Physical Property Estimates

A reliable measure of seismic properties as a function of depth is a comprehensive and accurate method to appraise site characteristics above the abandoned Pb-Zn mines under U.S. Highway 69 near Treece, Kansas. Stiffness and stress build-up are good estimators of failure potential and associated risk of significant ground movement above the water-filled mines (Figure 9). Proven correlation between seismic properties and stiffness/rigidity was the basis for the highly detailed measurements of the seismic wavefield in materials above the voids at this site that could potentially be under elevated stress (Figure 10).

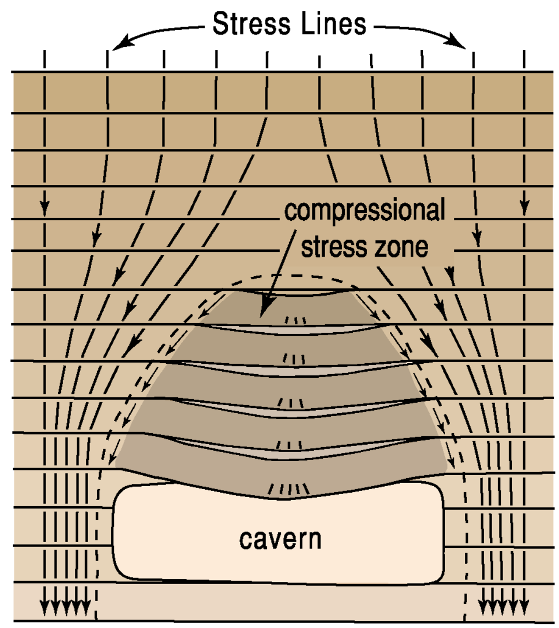

Figure 9. Tension dome and distribution of stress lines around a cavern opening in horizontal strata (modified from Davies, 1951).

In general, a seismic-reflection survey measures the elastic-wave propagation travel time between the source location and an interface. These interfaces are defined by their difference in acoustic impedance, which quantifies how much wave energy is being reflected or refracted at that point. Given these estimated travel times and seismic velocity of the material, the raypaths can be reconstructed to produce 2-D sections of reflections that represent stratigraphical and geological structure patterns (Sheriff and Geldart, 1995). As the complexity of the geologic environment and the surface noise increases, reflection events become more difficult to resolve and more advanced signal processing techniques are required. These complexities are demonstrated by heterogeneities such as faults or fractured rocks that interrupt the expected propagation direction of the wave.

The strength of individual rock layers can be qualitatively described in terms of stiffness/ rigidity and empirically estimated from measurements of the shear-wave velocity. Shear-wave velocity is directly proportional to stress and inversely related to non-elastic strain (Figure 10). Since the shear-wave velocity of earth materials changes when the stress and any associated elastic strain on those materials becomes “large,” it is reasonable to suggest load-bearing roof rock above mines may experience elevated shear-wave velocities due to loading between pillars.

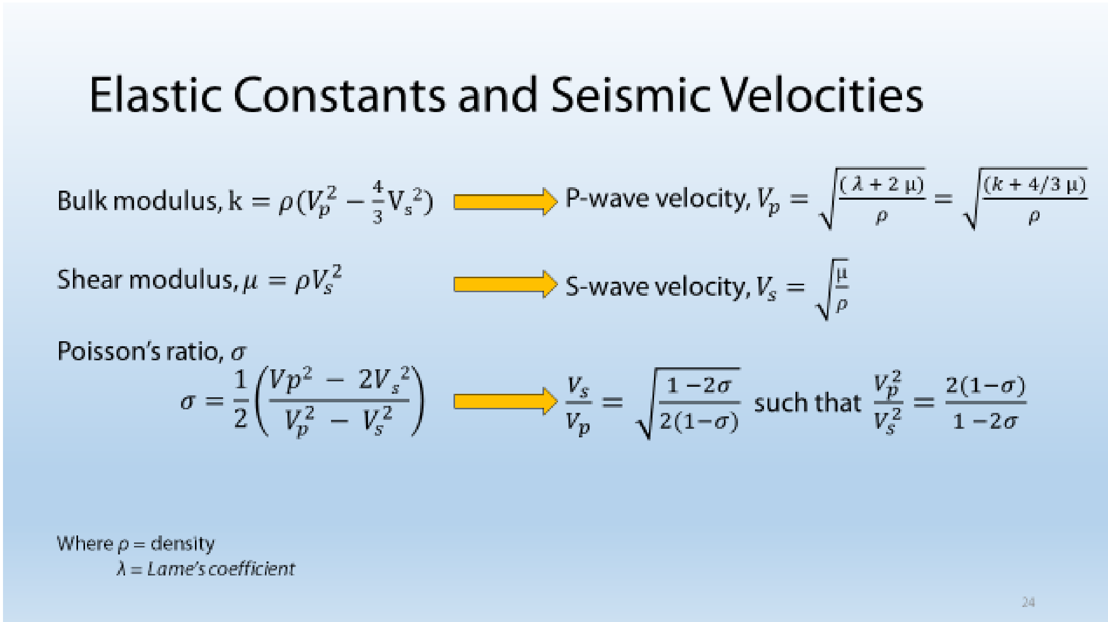

Figure 10. Relationship of seismic velocities with compressibility (bulk modulus), rigidity (shear modulus), and Poisson's Ratio (Sheriff and Geldart, 1995).

This localized increase in shear velocity is not related to increased strength, but increased load. High velocity shear-wave "halos" encompassing low velocity anomalies are key indicators of near-term roof failure.

Localized anomalous zones within otherwise laterally uniform earth materials disrupt the propagation pattern of the seismic wavefield. The degree of disruption and components of the wavefield that are altered depend on the material type, depth, and dimensions of the anomaly and properties of the surrounding host rock. Key to interpreting on seismic data whether these anomalies are geologic in nature (boulders, faults, fractures, erosional features, etc.), infra-structure components (culverts, buried trenches, footings, buried walls, etc.), or voids (tunnels, mines, caves, etc.) revolves around discriminating how each energy mode has been affected and classifying each anomaly based on interpretations of individual components of the seismic wavefield (Figure 11). Coincident interpretation of the components of the seismic wavefield dramatically reduces nonuniqueness and, therefore, improves target detection confidence and enhances the potential for a more automated system.

Surface-wave and body-wave energy components of the wavefield are affected to some degree by these localized anomalous zones. Disturbances in the wavefield of this type alter the dispersive characteristics of the surface wave and the travel time and propagation pattern of body waves. Based on the phase or moveout velocity, time, and location of the backscattered, diffracted, or reflected event, the anomaly can be located with reasonable accuracy in a specified earth volume. By analyzing changes in the propagation patterns of the entire wavefield, seismic anomalies related to voids, changes in material composition or structures, anthropogenic features, and even variation in bedrock depths can be ascertained.

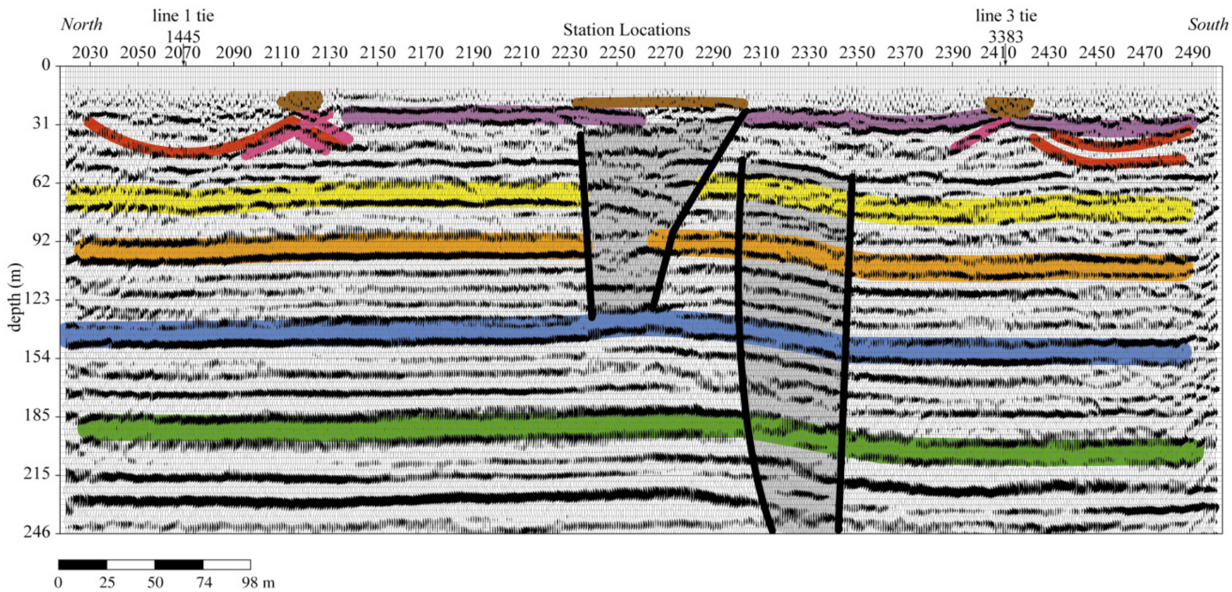

Figure 11. CMP stacked section over karst subsidence feature and fault bound monocline. Diffraction scatter events are evident as well as collapse structures infilled with alluvium post collapse and subsidence. These are the kinds of features expect around slump pipes in this area.

Subsidence-prone areas with limited subsurface control, significant velocity contrasts between affected and unaffected rock/sediment units, and gradual or segmented roof failure are especially suited targets for surface-wave imaging (Figure 12). Key indicators of either subsidence activity or areas with a strong potential for roof collapse are lateral decreases in the shear-wave velocity related to changes in fracture density with localized increases in shear-wave velocity defining the tension dome and increased stress surrounding the roof of cavities (Sloan et al., 2009).

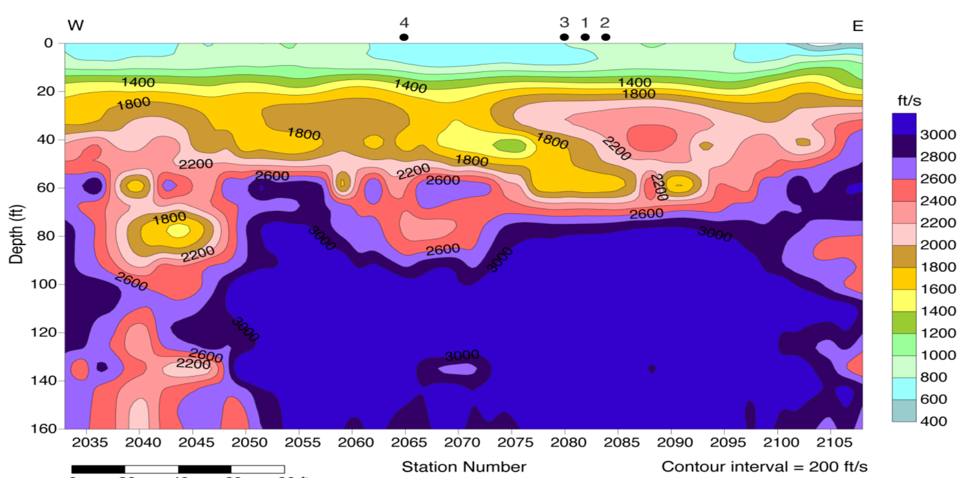

Figure 12. MASW cross section from south of Baxter Springs, Kansas, over an abandoned Pb-Zn mine with drift extending under State Line Road. Mine drift was determined from maps and drilling located at station 2045 at around 80 ft below ground surface.

Several key characteristics of surface waves and surface-wave imaging make application of this technique possible in areas and at sites where other geophysical tools have failed or provided inadequate results. First, and probably foremost, is the ease with which surface waves can be generated. The relative high amplitude nature of surface waves (in comparison to body waves) makes their application possible in areas with elevated levels of mechanic/acoustic noise.

Acquisition and analysis of the full seismic wavefield along continuous 2-D traverses passing over the target area focused on detection, isolation, and enhancement of waveforms and propagation patterns inconsistent with the native, local geologic setting and consistent with seismic signatures of voids and mine structures. Body-wave (compressional and shear) raypaths (reflected, refracted, and diffracted) and surface-wave energy (ground roll—fundamental and higher modes) raypaths (linear dispersive, reflected, and diffracted) are separated and analyzed to extract energy arrival patterns, phase velocity, amplitude, and frequency. Awareness of the power of interpreting change in the subsurface as opposed to directly classifying seismic anomalies dictates that an optimized approach to differencing/time-lapse analysis be formulated that focuses on dynamic anomalies.

Surface-wave Background

Surface waves are a type of high-amplitude seismic wave that propagates along a free surface and are characterized by their frequency-dependent dispersive behavior through a medium with a vertical velocity gradient (Park et al., 1999). Shear-wave velocity profiles calculated from surface-wave data have been increasingly used to aid and support environmental and engineering applications, in part because of the direct relationship between shear-wave velocity and the shear modulus (Figure 10) (Sheriff and Geldart, 1995). Surface-wave seismic imaging has been used to effectively map bedrock surfaces at depth (Miller et al., 1999), locate faults and fractures (Ivanov et al., 2006), and identify dissolution features (Miller et al., 2005; Sloan et al., 2009). Although surface-wave methods have successfully imaged to 100 ft, the attenuation of dispersion energy is greatly influenced by *in situ* conditions. If low-velocity or high-attenuating features (e.g., weathered materials) exist in the subsurface, surface-wave energy may decay more rapidly and subsequently affect the depth of investigation.

Two surface-wave methods were used to produce images the upper 100 ft of U.S. Highway 69. The first method, the multichannel analysis of surface waves (MASW) method, uses multiple receivers (i.e., geophones) evenly distributed along a linear array (Park et al., 1999) to measure surface-wave energy that can be inverted to estimate subsurface shear-wave velocities (Vs) as a 1-D or 2-D profile.

The MASW method can be summarized in three steps: (1) collect surface-wave data (Figure 13a), (2) extract dispersion curves, and (3) invert dispersion curves for 1-D Vs profiles (Figure 13b) that may be combined to form a 2-D section (Figure 13c). A dispersion curve is a picked set of values that illustrates the relationship between phase velocity and frequency providing non-unique velocity-depth information after inversion. For the purpose of this study, fundamental-mode Rayleigh-wave energy was used to generate dispersion images. Information about the overall soil structure and stress field was interpreted from differences or changes in Vs observed throughout the survey area.

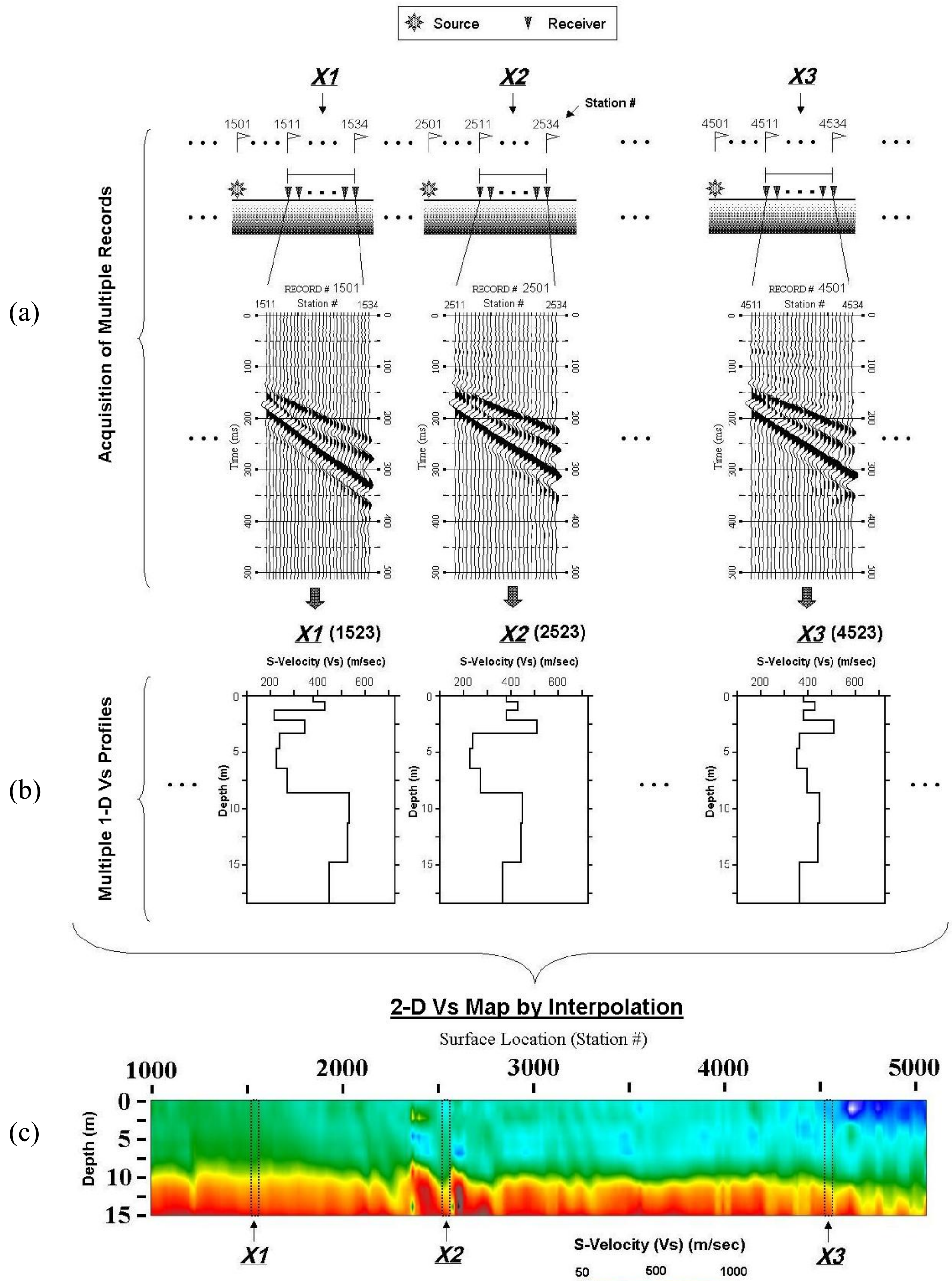

Figure 13. (a) Multiple records are acquired during an MASW using the same source offset with each new source location along the profile. (b) Dispersion curves are picked, extracted, and inverted to produce a 1-D Vs profile for each record. (c) 1-D Vs profiles are compiled into one 2-D image to create a vertical slice of the imaged subsurface (Ivanov et al., 2013).

The second method, the horizontal-to-vertical spectral ratio (HVSR), utilizes single 3-component (3-C) seismometers and passive Rayleigh-wave surface waves to measure the natural resonance frequency of soil overburden (Bonnefoy-Claudet et al., 2006). Soils exhibit a natural resonance frequency (Figure 14) related to the thickness of the soil column over rock that, if exposed to increased levels of ground motion, can lead to failure (Nakamura, 2009). The natural resonance frequency, f_0, can be used to estimate the depth-to-bedrock, z, or the average velocity of the overburden, V_s, using equation 1 if a 2:1 velocity contrast exists between the overburden and the underlying bedrock.

$$V_s = 4zf_0 \qquad \text{(Eq. 1)}$$

Since numerous boreholes are present throughout the field site, depth-to-bedrock (i.e., shale) is known. Therefore, the weathered state of the shale can potentially be evaluated by estimating the average velocity and comparing the result to that expected for the materials for the reported thickness. If the average velocity is higher than anticipated, then the weathered shale may not be providing a large enough contrast between that and the above silty clay.

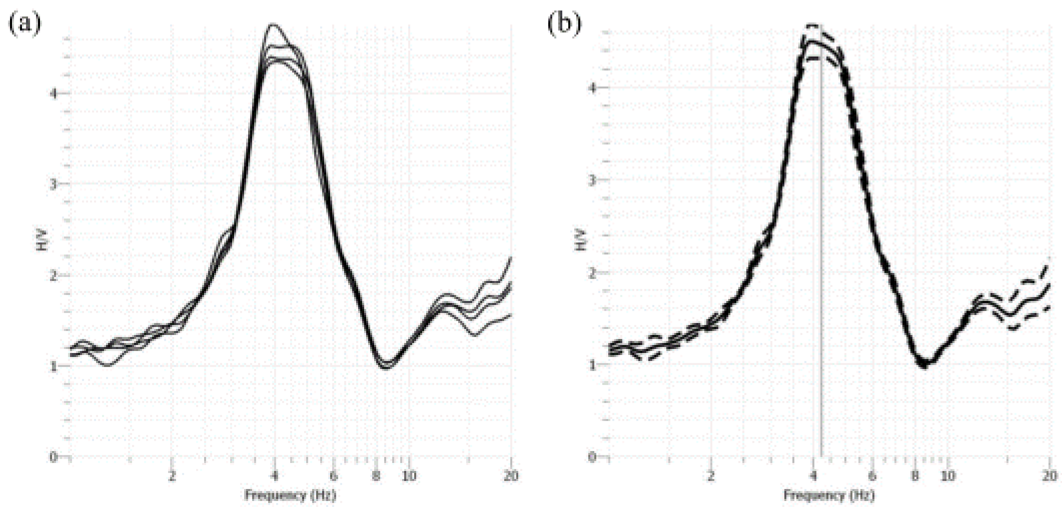

Figure 14. Example resonance frequency curves where the vertical axis is the amplitude ratio of the east and west horizontal components to the vertical components of measured surface waves (Morton, 2014).

Reflection Data Acquisition

The Kansas Geological Survey Exploration Services group (KGS) in conjunction with the Kansas Department of Transportation (KDOT) collected two high-resolution seismic reflection data sets over the course of two trips for a total of eight days (Table 2). Field conditions for both trips were ideal, with temperatures ranging from 70 to 86 degrees Fahrenheit, minimal wind (< 5 mph), and dry air, which allowed for optimal geophone coupling with the ground. Necessary precautions in the field were taken during acquisition to minimize recording of vehicle noise (i.e., highway traffic and nearby road construction).

Table 2. Reflection Survey Acquisition Comparison: P-wave vs. S-wave

	P-wave	S-wave
Date	August 2015	June 2016
Length of Profile	1.5 miles	1 mile
Frequency Sweep	25-300 Hz	15-150 Hz
Receivers	(3) 28 Hz vertical geophones	(1) 14 Hz horizontal geophones
Source Spacing	16 ft	16 ft
Receiver Spacing	8 ft	8 ft

P-wave Data Acquisition

The 1.5-mile compressional-wave survey was acquired using a 600-channel rolling fixed-spread geometry. An array of three Sercel 28 Hz geophones (Figure 15a) were planted at intervals of 8 ft. Geophones were planted in the west ditch in hard soil using 3¼” spikes for improved coupling to the surface. Frictionally coupled rock plates were used in place of spikes for sections of the seismic line that crossed hard surfaces (i.e., intersections and in areas with road construction). The seismic source, an IVI Minivib 1, delivered three 10-second, 25-300 Hz linear upsweeps with a 1.5-second taper at each source station (Figures 16a and 16b). Source stations were spaced 16 ft apart, coincident with every other receiver station, along the paved southbound highway shoulder. To increase fold, source stations began 165 ft south of the first receiver (near the OK/KS border) and moved northward into the spread. Twenty-five 24-bit Geometrics Geodes were used for recording data, resulting in up to 600 traces recorded for each sweep (Figure 14b). The first trace in each shot record was a synthetic pilot trace and the second trace in each record was the ground force pilot, transmitted via radio telemetry from the source to the seismograph. Each sweep was recorded and stored uncorrelated to allow follow-up pre-correlation processing. A GPS data point was taken at every receiver location to ensure consistency for future surveys and accuracy during data processing.

Data were acquired with a rolling fixed-spread geometry. As the Minivib moved through the fixed receiver spread, receivers from the farthest offsets behind the source were “rolled” to the front of the line once the source moved past half way into the receiver spread. Once the sensors from the back of the spread were moved to the front, a new fixed spread was defined

(a) (b)

Figure 15. (a) Three 28-Hz P-wave geophones were planted every 8 ft along U.S. Highway 69. (b) Data collection was controlled by a Geometrics 600-channel seismograph inside a John Deer Gator.

(a) (b)

Figure 16. (a) A Minivib 1 Vibroseis source was used with (b) a plate to induce P-wave energy with a linear up-sweep.

relative to the source. U.S. Highway 69 was open and moving heavy traffic volumes the during data collection. KDOT staff controlled both volume and speed of traffic flow by closing the southbound lane—which was occupied by the Minivib—and using a pilot car to guide one-way traffic along the northbound lane. Well locations were correlated to receiver stations and located using GPS data points to allow for an integrated interpretation of seismic with well data. Field notes also documented dead phones, culverts, and shot stations that were not collected to allow for detailed and accurate preprocessing.

During the survey, the total number of recording channels varied between 600 and 456 at different points along the profile, all the time being vigilant about optimum recording offsets. This slight variation in total receiver count had no impact on the resulting 2-D reflection profiles.

S-wave Data Acquisition

The 1-mile shear-wave survey was acquired using a 612-channel rolling fixed-spread geometry. One Geospace 14-Hz shear-component geophone was planted in an S_H orientation at each receiver station, each separated by 8 ft. Geophones were planted in the west road ditch in hard soil using ~3" spikes for improved coupling to the ground surface. Rock plates were again used for the portions of the line crossing hard surfaces. Source stations were spaced every 16 ft along the paved southbound highway shoulder. Source stations began at the first receiver station near the OK/KS border. An IVI Minivib 1 with the mass rotated to an S_H configuration was the source, and imparted three 10-second, 15-150 Hz linear upsweeps with half-second tapers at each source station (Figures 16a and 16b). Twenty-six 24-bit Geometrics Geodes were used for data collection, resulting in up to 612 recorded traces for each shot (Figure 13b). The third trace in each shot record was the ground force pilot telemetered from the vibrator to the seismograph, and the fourth trace recorded the source energy. Traces one and two were auxiliary traces not in use. Each sweep was recorded and stored uncorrelated, allowing for post-acquisition enhanced pre-correlation processing.

As the Minivib moved through the 612-channel fixed spread, 24 receiver stations were incrementally rolled from the back to the front of the line. The Minivib occupied the southbound lane, and KDOT controlled traffic flow along the northbound lane. All well locations were annotated in the field notes to allow for interpretation and correlation with P-wave seismic data and well data. Dead phones, culverts, and unused shot stations were logged in field notes to allow for detailed and accurate preprocessing and ground truth correlations during interpretations. It was determined through analysis of the P-wave data set that a shorter 1-mile survey line would still allow for complete imaging of the mine.

Seismic Reflection Data Processing

All seismic data were processed using proprietary software developed at the KGS, including SeisUtilities, LWSeis, WinSeis, and SurfSeis. Surfer (from Golden Software) was used for generating the velocity map based on the velocity model developed using several different KGS software components. P-wave and S-wave data were processed generally following 2-D high-resolution CMP processing approach (Steeples and Miller, 1998; Miller, 2007). The processing workflow and parameters were specifically tuned for each individual data set. All data were stored in industry standard SEG-2 format.

P-wave Data Processing

The processing workflow followed to generate the final P-wave CMP-stacked section was similar to workflows proven in near-surface seismic-reflection imaging. The combination of pre-processing steps, including vibroseis whitening (VSW), trace editing, and vertical stacking of shot records, helped suppress noise, removed unwanted energy, and optimized signal-to-noise ratio (S/N). Due to the complexity of the structurally altered subsurface, lack of lateral uniformity in material, and irregular mine geometry, the data were inherently noisy. High-amplitude, low-frequency coherent energy (predominantly from the upper tens of feet) and traffic noise was present throughout the data. FK filtering, combined with spectral balancing and additional frequency filtering (bandpass and low-cut), attenuated much of the unwanted surface-wave amplitudes, enhanced frequencies, and flattened the spectrum throughout the data set. This sequence of processing steps suppressed cultural noise and surface waves, which allowed further noise suppression, thus aiding in the identification of reflections in the shot record. First-arrival and surgical cone muting removed additional unwanted energy caused by first-arrival, ground roll, and air-wave energy.

Normal moveout (NMO) corrections were applied using stacking velocities ranging from 5250 ft/s to 9430 ft/s that were calculated using constant velocity stacks, semblance analysis, and curve fitting on shot gathers. This velocity range is reasonable for the lithologic intervals and the structural alterations documented in this vicinity. Velocity analysis was combined with automatic surface consistent statics to generate a representative common midpoint stack. A high-cut frequency filter was applied to the CMP stacked section to reduce ambient noise in this stacked section. An FK migration filter was also used to improve reflection wavelet coherency. Finally, the optimum velocity function was used to produce a depth-converted stacked section. AGC was then applied to the migration-filtered depth-converted stacked section to improve the S/N and interpretability of the 2-D seismic cross sections (Figure 17).

S-wave Data Processing

Although the S-wave data processing followed a workflow similar to that used with the P-wave data, the workflows were not identical as should be expected considering the different characteristics of the two modes. Overall, the shear-wave dataset was plagued with lower signal-to-noise ratio than was the P-wave. Preprocessing steps were reasonably consistent with the P-wave data set, including VSW, cross correlation, geometry, trace editing, and vertically stacking all three shot records. These steps reduced coherent noise produced by traffic, construction, field crew movement, etc., and increased the S/N by suppressing the most prominent noise. Spectral balancing, bandpass, low-cut and high-cut filters were methodically applied to suppress spectrally unique aspects of the noise outside the reach of surgical editing. First-arrival and inside cone mutes were designed and applied to remove coherent noise such as first-arrival energy, air-wave, ground-roll, and surface-wave energy that could not be attenuated through aggressive filtering.

A complex velocity function was defined using a variety of analysis techniques, but principally from constant velocity stack panels. From those panels NMO stacking velocities ranging from approximately 3280 ft/s to 6235 ft/s were assigned to CMP time series traces at 25 CMP intervals. An enhanced velocity function was defined using an iterative combination of automatic surface-consistent statics and velocity analysis. This approach resulted in the most representative stacked section possible for these data. Finally, FK migration was performed on the data to generate a final depth-converted stacked section (Figure 18).

P-wave Reflection Results

Reflection events with the greatest coherency and S/N ratio are at the north end of the interpreted P-wave section and depict the Miami trough at CMPs 3200 to 3975 (Figure 19). As expected (McKnight and Fisher, 1970), the center of the Miami trough is approximately 300 ft BGS where the seismic profile crosses this regional structure. A southward dipping normal fault at CMPs 3170-3175 bounds the southern end of the trough and likely played a role in establishing the northern extent of the mineralization zone. The interpreted green reflection interval is

Figure 17. Final P-wave stacked section.

Figure 18. Final S-wave stacked section.

within a limestone interval of the Mississippian Boone Formation, which is overlain by shale units representing bedrock and confirmed with shallow drilling. The shale interval representing bedrock was above the time interval imaged by these data. This shallowest imaged limestone contact can be correlated across the section from the northernmost point (CMP 3980) southward across the fault to a point it becomes difficult to distinguish from other coherent seismic arrivals. This loss of coherency, due to diminishing lateral continuity and decreased S/N, occurs around CMP 3100. Coherent reflections at approximately 250 ft BGS from CMPs 2830 to 2900 appear to terminate as they approach the mine area, an observation consistent with drill data.

There are no coherent and continuous P-wave reflections that appear to be associated with or interpretable as the mine roof. However, lithologic contacts encountered in wells along the seismic profiles were a challenge to correlate with apparent reflections on the CMP-stacked seismic data. This observation supports the suggestion of an absence of laterally continuous and coherent reflectors at or above the mine roof between approximately CMPs 2370 and 2755. The surface extent of the mine is defined on the stacked sections by the area highlighted in blue (Figure 19).

Diffractions, traced on the stacked sections in red (CMPs 2275 to 2670), are evident throughout the volume above the mine (Figure 19). Diffractions are a product of point source scatter generally resulting from the seismic wavefield encountering fractures, faults, abrupt layer terminations such as mine features (walls and pillars), and bed terminations. A mine pillar is interpreted on the stacked section based on the character of a diffraction set in conjunction with well data. This particular feature is highlighted in orange and is associated with a small area of coherent reflection between approximately CMPs 2555 and 2585. It must always be kept in mind that any interpretation based on geophysical data alone or in conjunction with one-dimensional well data is nonunique and could be the response from many different features or settings.

A packet of disturbed reflections that lack lateral consistency and are interfered with by a diffraction south of well 1 could support the notion that the mine (or at least the fracture/fault sequence being mined) extends further south than previously projected on mine maps. Based on all available published data, it is not clear if the mine could extend further south beneath the road as suggested by the seismic reflection data. Alternately, the more chaotic nature of the seismic data across the southern portion of the line could, wholly or in part, be the result of out-of-the-plane reflections. The three-dimensional nature of the mine and associated geologic structures would be a prime generator of out-of-the-plane energy.

The significance and source of the laterally consistent green layer, shown to extend the entire length of the seismic line, must be interpreted with caution. The coherency of this event is sufficiently high to allow it to be followed from the north end of the line to near the northern extent of the mine. It is difficult to suggest this green reflection event extends through the mine area and into the southern portion of the line. From the well data we expect a contact with a limestone unit associated with the Boone Formation to be continuous across the site and of sufficient reflectivity to represent a marker reflector.

Figure 19. P-wave interpreted section.

Overall the stacked section lacks the kind of uniform, lateral consistency commonly observed in interpretable reflections from exploration seismic surveys. No doubt, the majority of the very inconsistent reflections is due to the nature of the disturbed subsurface and associated reflectors that provide the host for the economic mining activities prevalent during the turn of the twentieth century. P-wave stacked sections at various stages of processing consistently depict the subsurface as highly altered, with most structures influenced by fractures and faults. Diffractions are a principal coherent component of the data. These diffractions could be indicative of many subsurface or surface features, but the most likely in this setting are rock intervals that are disturbed by dense complexes of fractures or faults. The irregular nature of mine drifts known to exist at this site from drilling and mine maps, in conjunction with the highly altered state of overlying roof rock, are very likely responsible for the lack of coherent reflectors above the mine.

The northern portion of the line has laterally continuous reflections that are likely associated with reflectors associated with the Miami trough. These geometrically diagnostic reflectors (defined by the reflections on CMP stacked sections) appear to stop abruptly in proximity to the northern extreme of the mine area. This further supports the suggestion that the mine area lacks layered/continuous reflections due to altered roof rock and mine geometry that inhibit the recording of trace-to-trace coherent reflections. Interpretable reflection energy appears limited to depths less than approximately 650 ft BGS. Events below this appear chaotic, making it difficult to confidently interpret reflection events any deeper. Again, this is due to the extremely altered near-surface geology. The higher quality of the stacked section north of the mine allows interpretation of shallow layers within the Miami trough. Although not directly, reflections within the overburden help to define the expression of the mine with reasonable confidence.

S-wave Reflection Results

High amplitude reflections present in the vicinity of the mine around 200 ft BGS are interpreted as the contact of limestone and a water-filled void on the S-wave section (as shown on Figure 20 in blue). The mine roof is inferred from CMP stacked sections to span from CMP 2350 to 2750, which ties nicely with well data (Table 1). Reflections present in the data set range between 200 and 330 ft BGS at the approximate location of the mine. Correlating well data with reflections interpreted on the seismic line provides strong support for these blue highlighted reflections as consistent with the drill-confirmed depths of the mine roof. No void was encountered by well 5; this complete rock interval is interpreted as a pillar and is located at approximately CMP 2570 to 2590 on the stacked section. Considering the resolution and S/N in this area, it is not possible with these seismic data to determine the actual size of this pillar, only that a pillar is the likely reason a complete rock column was present in this borehole and the seismic data suggest an interval of coherent rock.

Reflections, in general, lose amplitude and lateral consistency on the northern (CMPs 2750 to 3175) and southern (CMPs 2025 to 2350) portions of the line. Reflections on the south end of the imaged section lack the lateral consistency observed on the north end and suffer from a higher percentage of high frequency noise and lower amplitude reflections. The area interpreted in green on the S-wave section correlates to a limestone unit interpreted within the

Figure 20. S-wave interpreted section.

Mississippian Boone Formation on the P-wave data. Pinpointing the exact location of the roof of the mine is not advisable due to error in picking velocities and data resolution (due to frequency and bandwidth), therefore the reflection is interpreted to be in the vicinity of the mine as opposed to a return from the mine roof. The high-amplitude reflections associated with the mine are no doubt a result of the large acoustic impedance contrast the rock–water-filled void contact represents.

The structurally complex subsurface that was critical for hosting the extensive mineralization and made mining economical at this site also created a chaotic environment that scattered energy and inhibited the reflection arrivals from stacking coherently. As a result, accurate interpretation of specific rock units identified in boring data was difficult on the seismic sections. The key and objective of this stacked section was the interpretation of a reflection associated with the mine.

V_P/V_S Ratio

Vp/Vs ratio was calculated using the interval velocities derived from NMO velocities of the P- and S-wave data sets (Figures 21a and 21b). The Vp/Vs in the upper 490 ft BGS indicated no anomalous zones as defined by an excessive increase or decrease in the velocity ratio. More specifically, the upper 260 ft where the mine roof resides shows no zones of Vp/Vs ratio that would cause concern (Figure 22). The average Vp/Vs ratio of this unit and above is ~1.8, which falls within an expected Vp/Vs range for limestone (Yilmaz, 1987). The slight variation across the section for the limestone ranges from ~1.6 to ~1.9 and is due to small lateral variations in interval velocities inconsistent with loss of rock strength (Figures 21a and 21b). These values are well within an error range of velocity picking. This means that a slight change in the stacking velocities (±300 ft/s) could change this ratio to a more locally consistent single value such as 1.8. A reflection from the limestone unit is the most consistently identified in the two data sets and is the main focus of any rock strength study due to the depth of the mine roof. Fortunately, the Vp/Vs calculation does not suggest that any area of the mine roof represents a higher risk of failure than another. The relatively consistent values across the mine, as well as north and south of the mine, indicate that there do not appear to be any areas of increased stress at the time of these surveys. This being the first seismic data collected at this site allows these results to be used as an excellent baseline study. The Vp/Vs values calculated fall within a normal or expected range, but without a history of the rock properties above the mine we cannot say for certain that these values are native for this limestone. Changes of Vp/Vs in future surveys compared to this original data could imply changes of rock properties associated with increased or decreased stress over the mine void. As of this data collection in July 2016, there is no evidence supporting increased stress in overburden rocks in relation to the seismic velocities and rock properties within surrounding layers.

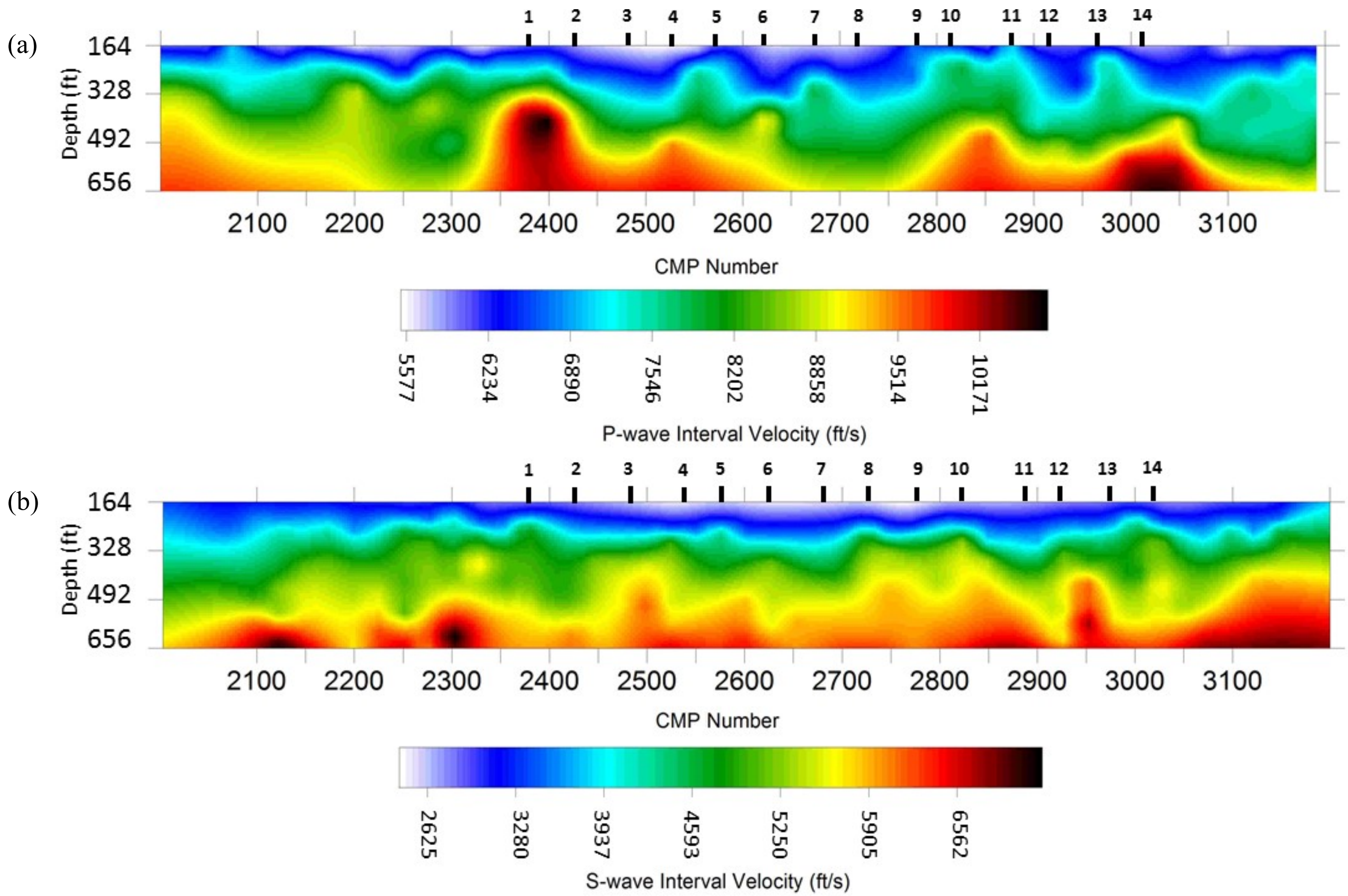

Figure 21. (a) P-wave interval velocity map with wells plotted at the approximate corresponding CMP. (b) S-wave interval velocity map with wells plotted at the approximate corresponding CMP.

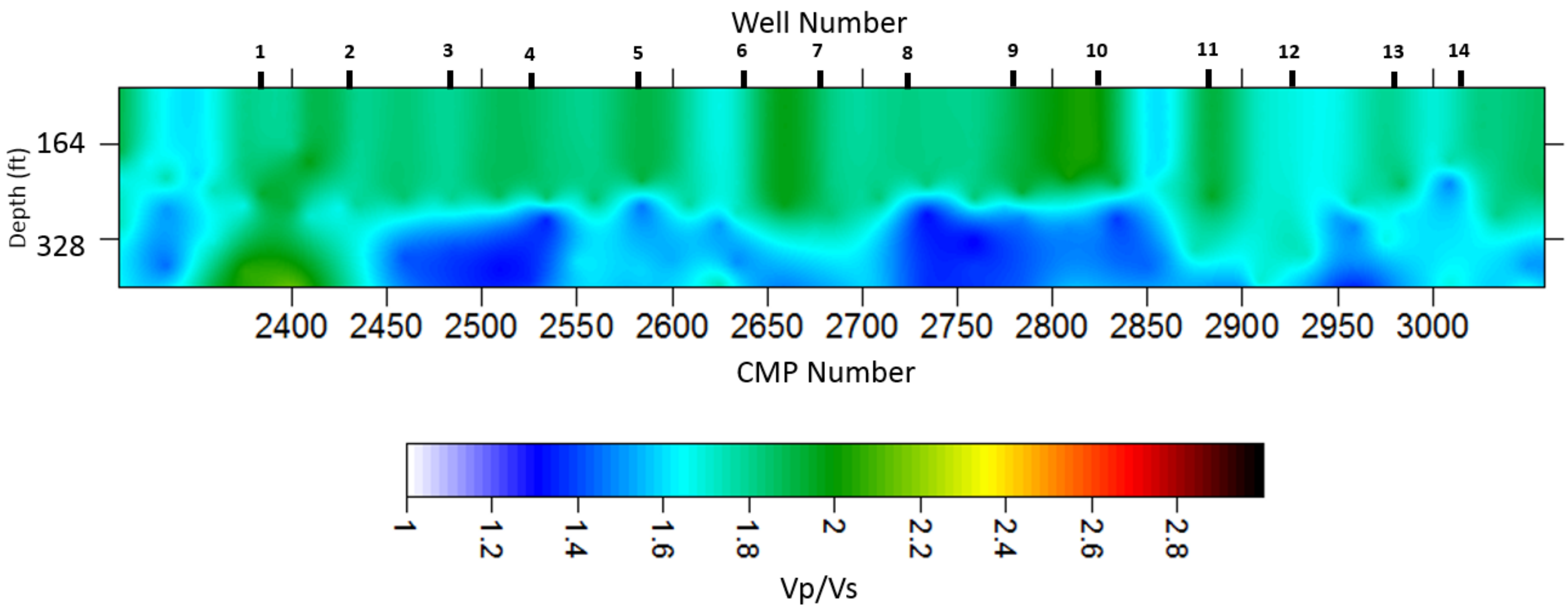

Figure 22. Calculated Vp/Vs using the interval velocities of the P- and S-wave data. On average, the upper 250 ft have a ratio greater than 2. This is due to an overall slower S-wave velocity at this depth because of the structurally altered limestone unit. The highest Vp/Vs are a result of increased P-wave velocities in areas where no mine is present, and is indicative of more competent rock.

Surface-wave Data Acquisition

For the active survey in June 2015, surface waves were generated using a vertically-accelerated weight-drop (AWD) source system that produced consistent and controlled seismic energy throughout the survey. The AWD was mounted to the front of the Toolcat vehicle (Figure 23a) that towed a land streamer (Figure 23b) with a 24-ft source-to-nearest receiver offset. The towed land streamer method was chosen instead of a fixed array because it requires less field support and time to acquire data, only a small portion of the survey area to be closed to traffic, and the length of the spread necessary for the MASW method is significantly shorter than that needed for reflection imaging.

Passive single-station seismic data were collected during November 2016 at acquisition points within 5 ft of wells 1-14 using a single Trillium 3-C seismograph at each wellhead (Figure 23c). Traffic along U.S. Highway 69 provided abundant passive or ambient surface-wave noise necessary for each 30- to 45-minute measurement.

Data acquisition and quality control for the MASW survey were monitored inside the Toolcat cabin equipped with Geometrics seismographs; acquisition parameters were determined based on previous experience. The firehose land streamer housed 48 receiver groups with 4.5-Hz vertical geophones at a 4-ft station separation. Each station coupled to the pavement surface using a three-rail metal skid plate. Three impacts were recorded at each source point. Source stations were on 8-ft intervals starting from the Kansas-Oklahoma border and progressing north on U.S. 69 past wells 1-14.

(a) (b) (c)

Figure 23. (a) A vertically-accelerated weight-drop source was used to induce active surface-wave motion. (b) A 48-receiver station land streamer was towed behind the Toolcat and contacted the pavement surface using metal coupling plates. (c) A 3-C seismometer on a metal plate was used to collect passive data at wellheads 1-14 throughout the MASW survey area.

Surface-wave Results

The scope of this project was to characterize the shallowest part of the overburden beneath U.S. Highway 69 above and in close proximity to an abandoned lead-zinc mine that was drill confirmed to be approximately 200-300 ft below portions of the highway (Table 1). The near-surface MASW Vs structure is consistent with relatively uniform layers of silty clay and shale down to 70-80 ft as logged in KDOT borings identified as wells 1-14 (Figure 24). Based on lost circulation and bit drop, the mine is located below wells 1-4, 6-8, 11, and 14 (Table 1). The MASW-produced velocity profile did not possess any anomalous features that would infer the upper ~80 ft above the mine was experiencing increased or decreased stress relative to off-mine areas as a result of elevated load or reduced strength due to roof failure at the time of this survey.

Shear-wave velocities ranged from 1600 to 2200 ft/s between 20 and 70 ft, and are reasonable for weathered and firm shale materials as reported in the geologic logs. Noteworthy is the observation that the extent of the weathered shale relative to firm shale appears deeper north of well 7 than noted in the geologic logs. This interpretation is made based on the variability of the Vs structure north of well 7 (Figures 24c-d). Surface-wave energy likely attenuated faster and subsequently reduced the depth of penetration due to the presence of this shallow (~20-30 ft) weathered shale. This lack of penetration depth is not likely related to changes in rock strength as much as changes in lithology across the profile. Due to a delay in acquisition of the passive single-station data, data processing is still ongoing and results will be reported in the future.

MASW processing was challenging along the southern portion of the line due to limited surface-wave penetration south of well 5. Data acquired in this section lacked dispersive energy below 20 Hz (Figure 25a) compared to north of this area where dispersive energy was observed down to 13 Hz (Figure 25b). This elevated lower frequency limit resulted in a 40 ft maximum depth of penetration. Additionally, shot gathers from southern stations (Figure 26a) display increased higher-mode amplitudes, effectively reducing the coherency of the desired slower fundamental mode energy in comparison to northern stations (Figure 26b). The KGS Seismic Team re-collected streamer data across this area in June 2016 to improve the penetration depths of the MASW results (Figure 27). The reacquired data provided adequate surface-wave energy penetration down to 70 ft. This additional 30 ft of imaging depth produced an image with a Vs structure consistent with that observed above well 5.

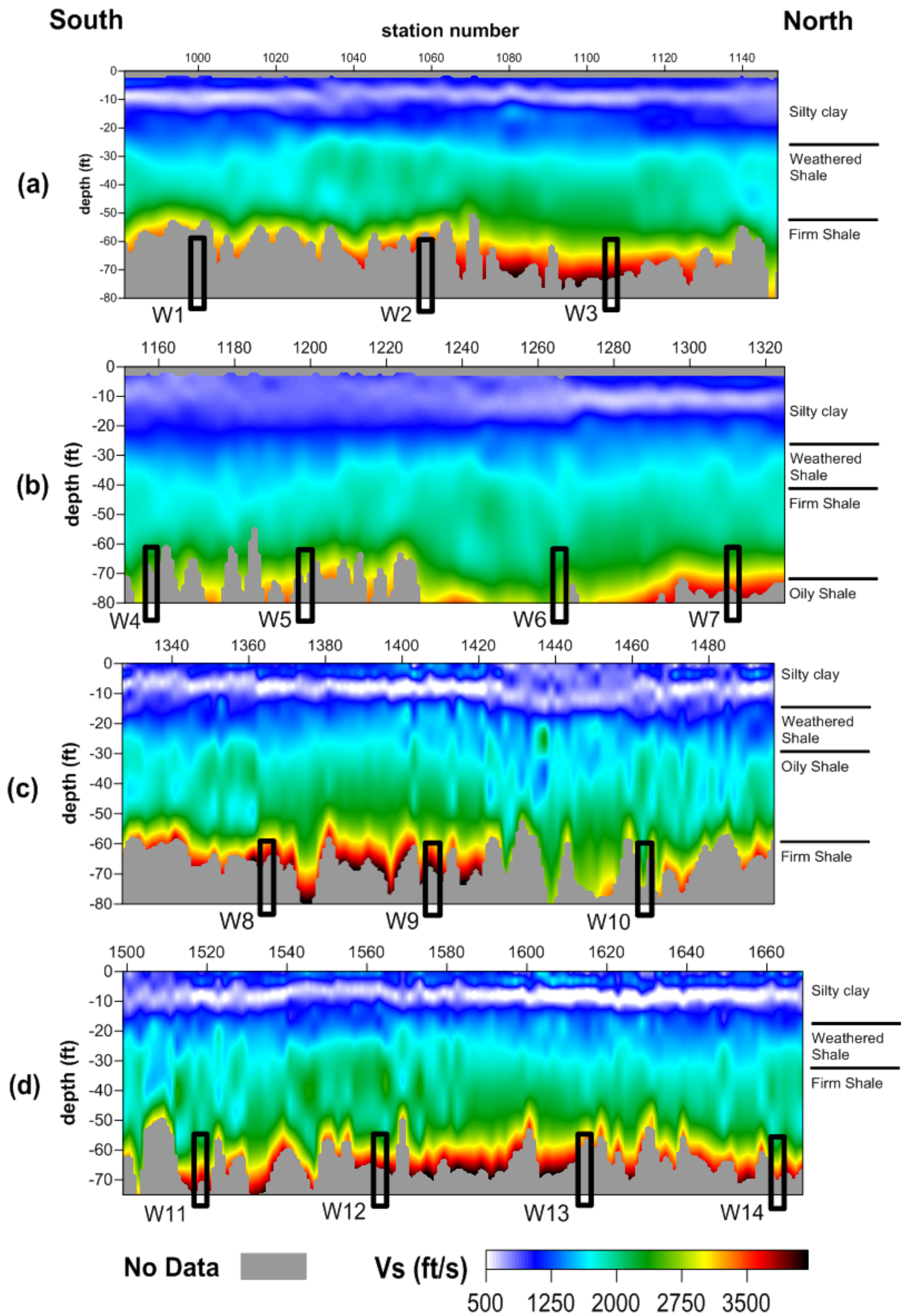

Figure 24. 2-D shear-wave velocity profiles were generated from mid-stations 985-1669. Velocity results shown here are supported by the fourteen borehole logs: silty clay from ~0-20 ft, weathered shale from ~20-30 ft, and firm shale ~30-80 ft. The mine is located below wells 1-4, 6-8, 11, and 14, but the Vs structure is relatively consistent throughout the entire profile.

(a)

(b)

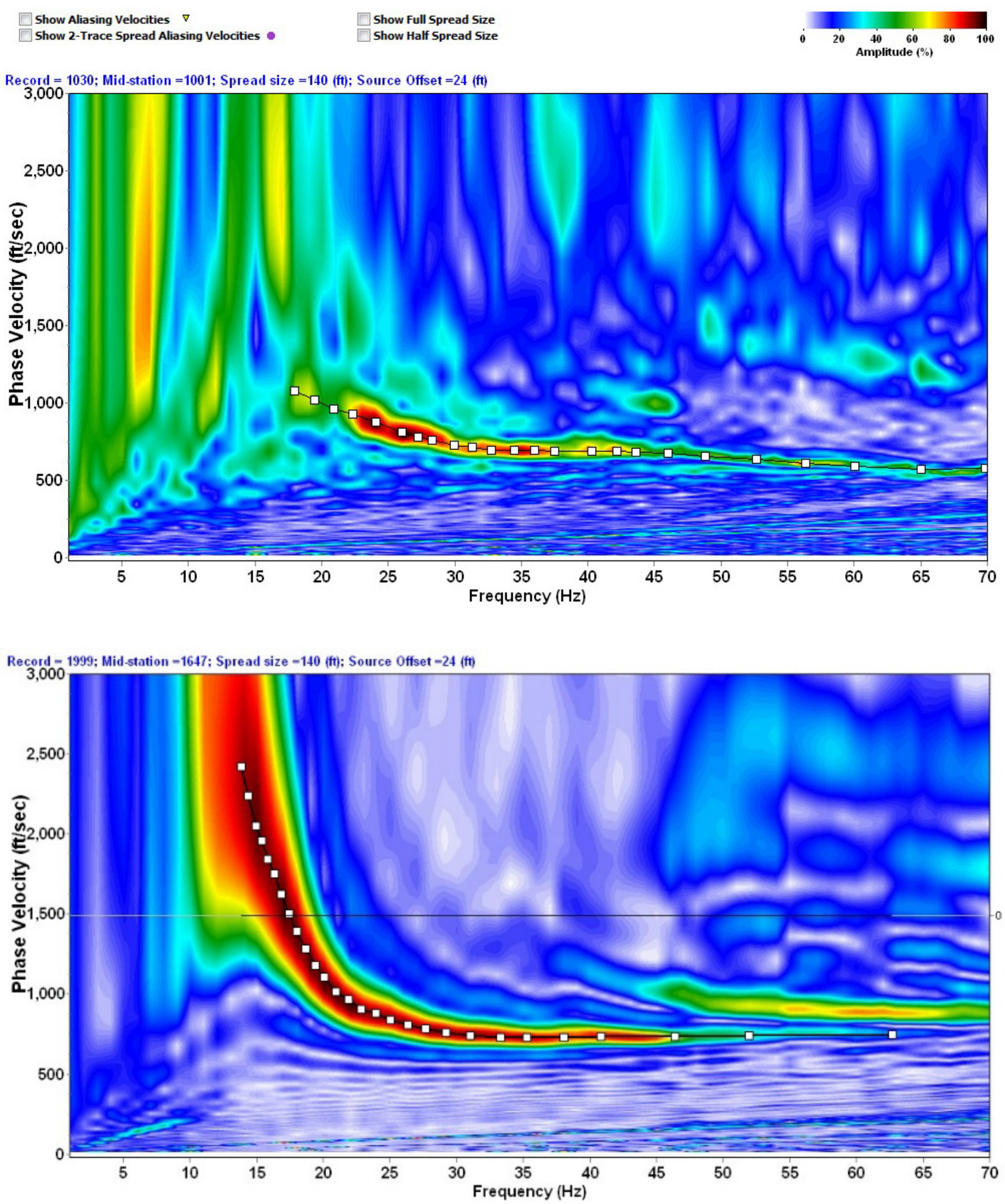

Figure 25. (a) Example picked dispersion curve from southern portion of the survey line that lacked low frequency energy below 18 Hz, limiting the depth of investigation in this area. (b) In the northern section of the line, coherent dispersion energy was observed down to 13 Hz, allowing deeper penetration depths (70 ft).

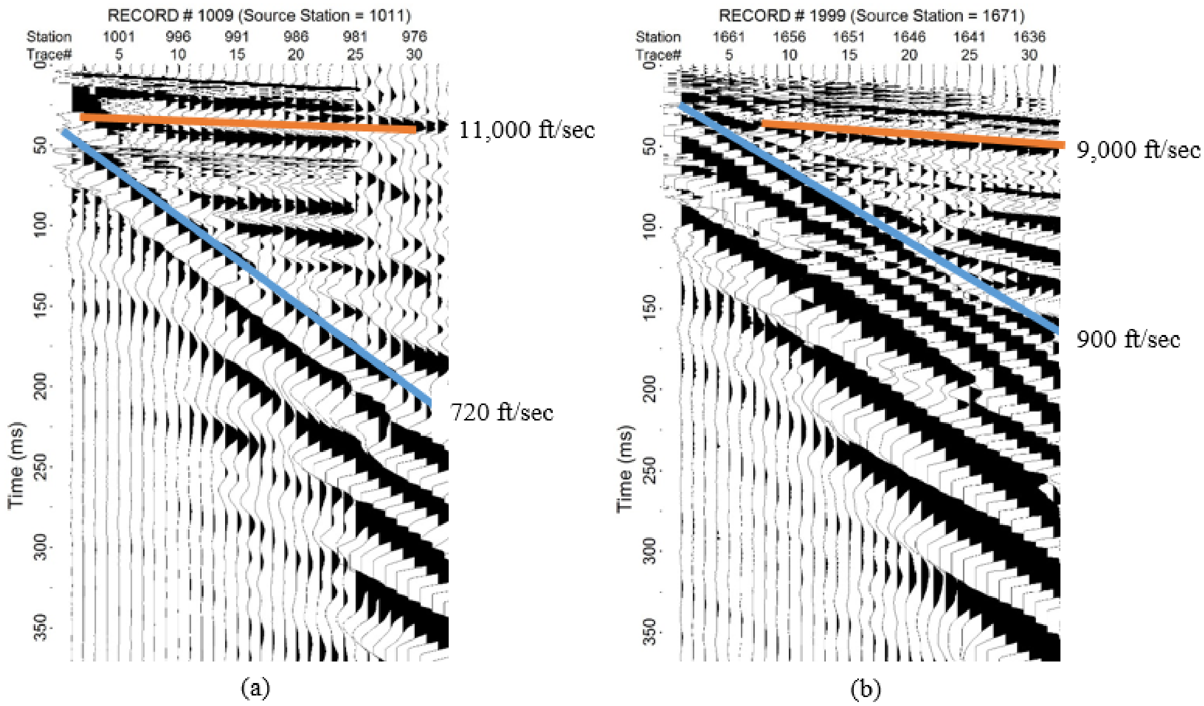

Figure 26. (a) Shot gather from southern portion of survey line where dominating higher-mode surface waves (orange line) reduced the coherency of the fundamental mode energy (blue line). (b) Shot gather from northern portion of survey line where fundamental mode amplitudes were less influenced by higher-mode surface waves and provided adequate low frequency information.

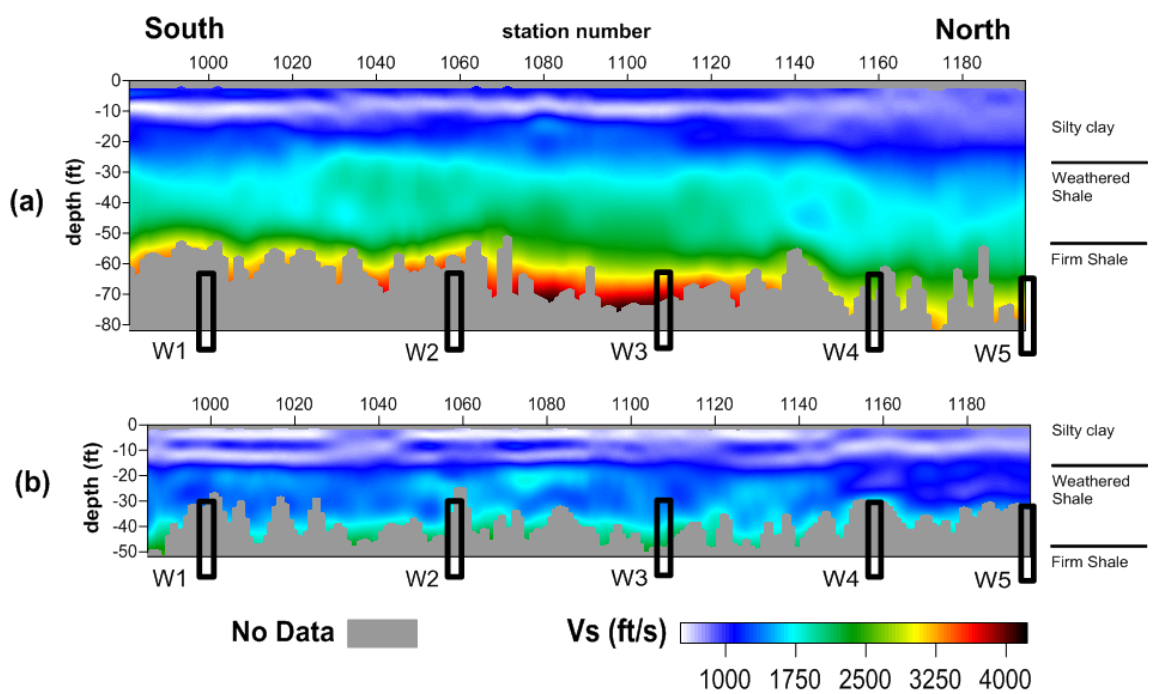

Figure 27. (a) 2-D Vs profile below well 5 collected in June 2016 achieved deeper depths of penetration (~70 ft) compared to the (b) July 2015 data that suffered below 40 ft.

Discussion

Compressional- and shear-wave reflection data sets are interpreted to possess a highly complex and altered overburden between the drill-confirmed roof of the mine and ground surface. A lack of lateral continuity across the entire 1.5-mile P-wave reflection profile (Figures 17 and 19) is consistent with a highly disturbed near surface exhibiting significant coherent energy contributions from both in and out of the 2-D imaging plane. Lack of consistency in reflection character above the mine location, as well as the presence of diffractions on the P-wave stacked sections (CMPs 2325 to 2650), suggests a more structurally altered overburden over the mine (e.g., faults, fractures), in comparison to the same units north of the mine (CMPs 2800 to 3957) that are outside the mineralized zone.

The mined interval (Boone Fm. Limestone) is at a depth of ~240 ft, which equates to around 75 ms. Tracking a reflection from within the host rock from the northern end of the P-wave stacked section to the KS/OK border (and southern end of the P-wave reflection profile) allows identification of mineralized zone or mine void as well as areas with structurally altered but more coherent reflection events. The most coherently imaged rocks are within the Miami trough and extend south from the northern extreme of the P-wave section to around CMP 2800, where highly altered reflectors begin to be evident within the mineralized zone. This is also evident in the S-wave stacked section (Figures 18 and 20). Although the S-wave section does not extend over the Miami trough, the change in character is evident at the north end of the profile. A high amplitude reflection in the S-wave data at CMPs 2350 to 2750 is interpreted based on wavelet character and location as the contact of limestone and water filled void (Figure 20), and this also matches the well data (Table 1). Unlike the P-wave stacked section, there appears to be enhanced trace-to-trace coherency in reflections at depths (200 and 330 ft BGS) consistent with the top of the mine. The characteristics of the shear-wave reflections change from laterally consistent, relatively high amplitude events over the mine to lower-amplitude, less-consistent events off the drill-confirmed mine roof.

Additionally, the surface-wave data provided a 2-D shear-wave velocity cross section of the upper 80 ft that is consistent with the lithology as described in the well borings. MASW results below well 5 suffered higher-mode attenuation that decreased the depth of investigation to 40 ft on the first survey. MASW data in the well 5 area reached depths greater than 80 ft after the line was reacquired in June 2016. Given the presence of clay and weathered shale within the upper 50 ft along this profile, surface-wave energy was expected to attenuate, but this extreme lack of penetration on the first data collected did not allow the goals of the survey to be met. For this reason, modifications were made during reacquisition of this section to compensate for the highly attenuative materials.

Overall, the seismic-reflection and surface-wave data sets were successful in determining the locations where the mine was present in the subsurface and indirectly the condition of the overburden. At this time, the seismic studies offer a solid foundation and appraisal of subsurface conditions at the time of this survey suitable for a time-lapse study where change in future surveys can be determined to a very subtle level. Changes in the S-wave reflection characteristics associated with the contact between the roof of the mine and water-filled void below would likely indicate an increased chance of localized failure over the mine. Increased disturbance in the P-wave reflection image—such as a higher number of diffractions present or a missing pillar at well 5 (CMPs 2560 to 2585) (Figure 20)—would be the kinds of structural changes that would justify invasive investigations to ascertain the source of the change.

In the upper 240 ft, Vp/Vs values were on average approximately ~1.8. No areas showed an increased or decreased value of Vp/Vs that appeared to be anomalous or inconsistent with the rest of the unit. The S-wave and P-wave velocities stay relatively laterally consistent across the profile from areas over the mine to areas north and south of the mine. Although the Vp/Vs did vary (~1.6 – ~1.9) for the overlying limestone unit, it does not vary enough to fall outside an error of velocity picking (Figures 19 and 20). Overall the Vp/Vs suggests the there are no major lateral changes in the rock properties, nor is any point over the mine at a greater degree of stress than another. The Vp/Vs calculation from these data provides another measure of the subsurface suitable for a baseline comparison for future surveys. Vp/Vs for these data are consistent with a stable overburden. Changes in Vp/Vs ratio in future data need to be dissected to determine if the change is due to increased P or S, or decreased P or S. Each has meaning that relates to the condition of the overburden.

Conclusion

The findings presented here are consistent with a snapshot in time of a stable overburden and provide an excellent baseline for future seismic investigations at this site. The interpreted seismic reflection sections indicate a lack of lateral consistency in certain lithologic units (i.e., limestones) in this area. These data also provide reasonable images of reflectors and velocity variability, allowing the presence of the mine to be inferred and correlated to well logs. The high-resolution seismic-reflection stacked sections combined with the Vp/Vs ratio map support concern for potential future sinkhole development. This data should be used as a baseline for future time-lapse comparisons. Surface-wave results provide no evidence of localized, elevated stress in the upper 80 ft that might be indicative of a weakening roof rock as of June 2016. Historically, roof rock failure around and at this site has proceeded both rapidly and gradually, depending on the size of the roof failure, depth below ground surface, and hydrology/lithology at and above the void. Whether the mine void reaches the ground surface will depend on the void's depth below ground surface, angle of draw, and bulking factor. Sinkhole development in this area would drastically threaten public safety and transportation.

Future monitoring is a reasonable plan of action to ensure public safety. Key findings presented here lend themselves to comparisons with future seismic investigation. A change in reflection character in the P- and S-wave stacked sections would lead to the assumption void migration may have begun. Increased Vp/Vs ratio, due to a decrease in Vs interval velocities relative to these baseline observations, could indicate a weakening in the overburden and a higher risk for gradual, vertical migration of the void. On the other hand, a lower Vp/Vs, due to increased Vs interval velocities, could indicate increased stress and increased opportunity for a more rapid failure scenario. At this time, the Vp/Vs indicates a stable environment above the mine, presuming the measured velocities are native values to these rocks. Without knowing if these are the native values, there is no way to confirm the observed stress is not greater than previous time periods; hence, future surveys are needed to provide an understanding of native at this location.

Recommendations include further monitoring of this site with combined P- and S-wave reflection- and surface-wave surveys. It is also recommended that density logs be performed at this site to allow for stiffness and rigidity to be estimated (Figure 10). The density values combined with Vs and Vp values will allow quantification of the overburden's elastic parameters, providing further insight into the integrity of the overlying units as well as the potential risk of increased structural weakening in this area.

References

Bonnefoy-Claudet, S., C. Cornou, P.-Y. Bard, F. Cotton, P. Moczo, J. Kristek, and D. Fäh, 2006. H/V ratio: a tool for site effects evaluation. Results from 1-D noise simulations: *Geophysical Journal International*, v. 167, p. 827-837.

Davies, W.E., 1951, Mechanics of cavern breakdown: *National Speleological Society*, v. 13, p. 6-43.

Hambleton, W.W., J.P. Lyden, and D.C. Brockie, 1959, Geophysical investigations in the Tri-State zinc and lead mining district, *in* W.W. Hambleton, ed., Symposium on geophysics in Kansas: Kansas Geological Survey Bulletin 137, p. 357-375. Available online at http://www.kgs.ku.edu/Publications/Bulletins/137/Hambleton/index.html

Ivanov, J., R.D. Miller, C.B. Park, and J. Xia, 2013, The MASW seismic method, What it is and how it works: Material prepared for SurfSeis/MASW course by the Kansas Geological Survey.

Ivanov, J., R.D. Miller, P. Lacombe, C.D. Johnson, and J.W. Lane, Jr., 2006, Delineating a shallow fault zone and dipping bedrock strata using multichannel analysis of surface waves with a land streamer. *Geophysics*, v. 71, n. 5, p. A39-A42.

Judy, B.E., 2015, High-resolution seismic reflection to characterize small scale mechanisms of large scale natural dissolution in the Hutchinson Salt Member: Master's thesis, University of Kansas Department of Geology, 95 p.

Kansas Department of Transportation (KDOT), 2009, Borehole report, US-69 Tomography, Project #K-6799-04, Sounding #6.

Lambrecht, J.L., 2006, Time-lapse high-resolution seismic imaging of a catastrophic salt-dissolution sinkhole in central Kansas: Master's thesis, University of Kansas Department of Geology, 80 p.

Luza, K.V., 1986, Stability problems associated with abandoned underground mines in the Picher Field, Northeastern Oklahoma: Oklahoma Geological Survey Circular 88.

McCauley, J.R., L.L. Brady, and F.W. Wilson, 1983, Study of stability problems and hazard evaluation of the Kansas portion of the Tri-State mining area (Contract 10100131 report): U.S. Bureau of Mines Open-file Report 75-83, 193 p. (Also Kansas Geological Survey Open-file Report 83-2.)

McKnight, E.T., and R.P. Fischer, 1970, Geology and ore deposits of the Picher Field, Oklahoma and Kansas: Geological Survey Professional Paper 588, U.S. Government Printing Office, http://pubs.usgs.gov/pp/0588/report.pdf.

Miller, R.D., 2007, High-resolution seismic investigation of subsidence from dissolution: Ph.D. dissertation, Montanuniverstät Leoben, Austria, 417 p.

Miller, R.D., D.W. Steeples, J.L. Lambrecht, and N. Croxton, 2006, High-resolution seismic-reflection imaging 25 years of change in I-70 sinkhole, Russell, County, Kansas [Exp. Abs.]: Annual Meeting of the Soc. of Expl. Geophys., New Orleans, Louisiana, October 1-6, p. 1411-1414.

Miller, R.D., A. Villella, and J. Xia, 1997, Shallow high resolution seismic reflection to delineate upper 400 m around a collapse feature in central Kansas: *AAPG Division of Environmental Geosciences Journal*, v. 4, n. 3, p. 119-126.

Miller, R.D., J. Xia, and C.B. Park, 2005, Seismic techniques to delineate dissolution features (Karst) at a proposed power plant site: Soc. Explor. Geophys., Investigations in Geophysics no. 13, Dwain K. Butler, ed., *Near-Surface Geophysics*, p. 663-679.

Miller, R.D., J. Xia, C.B. Park, and J.M. Ivanov, 1999, Multichannel analysis of surfaces waves to map bedrock: *Leading Edge*, v. 18, n. 12, p. 1392-1396.
Morton, S.L.C., 2014, Comparison of geophysically-derived and surficial sediment-based estimates of seismic risk in Hartford County, Connecticut. Master's thesis, Department of Civil and Environmental Engineering, University of Connecticut, Master of Science, 231 p.
Nakamura, Y., 2009, Basic structure of QTS (HVSR) and examples of applications. *Increasing Seismic Safety by Combining Engineering Technologies and Seismological Data*: Springer, p. 33-51.
Park, C.B., R.D. Miller, and J. Xia, 1999, Multichannel analysis of surface waves: *Geophysics*, v. 64, n. 3, p. 800-808.
Park, C.B., R.D. Miller, J. Xia, and J. Ivanov, 2000, Multichannel seismic surface-wave methods for geotechnical applications: First International Conference on the Application of Geophysical Methodologies to Transportation Facilities and Infrastructure, St. Louis, December 11-15, 2000.
Penumadu, D., and C. Park, 2005, Multichannel analysis of surface wave (MASW) method for geotechnical site characterization: Proceedings of the GeoFrontiers Conference on Earthquake Engineering and Soil Conference, Austin, Texas, January 23-26.
Seevers, W.J., 1975, Description of the surficial rocks in Cherokee County, southeastern Kansas: Kansas Geological Survey Geology Series No. 1.
Sheriff, R.E., and L.P. Geldart, 1995, *Exploration Seismology*, 2nd ed.: Cambridge University Press, Cambridge.
Sloan, S.D., R.D. Miller, J. Ivanov, J., and S. Walters, 2009, Shear-wave velocity as an indicator of increased stress and failure potential association with dissolution mining voids. Symposium on the Application of Geophysics to Engineering and Environmental Problems 2009, p. 363-372.
Steeples, D.W., and R.D. Miller, 1998, Avoiding pitfalls in shallow seismic reflection surveys: *Geophysics*, v. 63, n. 4, p. 1213-1224.
Steeples, D.W., and R.D. Miller, 1990, Seismic reflection methods applied to engineering, environmental, and groundwater problems: Soc. Explor. Geophys. Investigations in Geophysics no. 5, Stan H. Ward, ed., *Volume 1: Review and Tutorial*, p. 1-30.
Wichita Eagle, 2009, Town over mines could dry up soon. Photograph. http://www.kansas.com/latest-news/article1010282.html.
Weidman, S., 1932, The Miami-Picher Zinc-Lead District, Oklahoma: Oklahoma Geological Survey Bulletin No. 56, http://www.ogs.ou.edu/pubsscanned/bulletins/Bulletin56mm.pdf.
Williams, W.T., and W.F. Fredericksen, 1985, Mine subsidence report; Mine subsidence 1.1 miles north of the Oklahoma line on U.S. 69, Cherokee County: Kansas Department of Transportation report, December 1985.
Yilmaz, Ö., 1987, *Seismic Data Processing*: Tulsa, Society of Exploration Geophysicists.